

exist in the area of the lens, which will be discussed in a later section.

Concentration of the oil within the reservoir begins before the entire pore volume of the reservoir is contacted. For example, at 4.0 million years oil has just contacted the entire reservoir space but oil has concentrated to 53 percent saturation along the upper boundary. The effect is similar to the observed saturation distribution in the matrix unit, where the oil concentrates along the upper boundary rather than migrating into non-saturated portions of the matrix.

As time progresses, the lens continues to fill from the upper, upstream "corner". At 3.0 million years (Figure 6.1b), oil saturation has attained a maximum value of 49 percent along the top of the reservoir. The process of initial downstream filling and concentration, followed by concentration towards the upstream end of the reservoir, occurs because oil is retained in the reservoir at the downstream boundary by a combination of capillary and hydrodynamic forces.

At 5.0 million years the simulation had to be stopped because oil began concentrating at the downstream end of the flow domain. Past 5.0 million years, oil began to flow back upstream. This spurious concentration was caused by the inability of the oil to migrate further downstream due to the presence of the grid boundary. The results up to the start of the spurious accumulation remain valid.

The final saturation distribution is shown in Figure 6.1c. Oil saturation has reached 55 percent, the limiting value imposed by the relative permeability curves, along the top 5.0 metres of the reservoir. Elsewhere in the reservoir, oil saturation varies from 38 to 55 percent.

Differential concentration of the oil is evident in the horizontal direction. Combined with the already existing vertical segregation, this produces tilted iso-saturation lines within the reservoir (Figure 6.2). The maximum oil saturation is observed at the upper, downstream position in the lens, with saturation values decreasing rapidly in any vertical section and less rapidly in any horizontal section.

Oil has continued to enter the lens upstream, but has started leaking out the downstream end. The downstream leakage occurs at a very slow rate. The net result is the observed, continued concentration within the reservoir. Oil saturations of up to 14 percent exist outside the reservoir because changes in fluid-potential conditions allow for some oil leakage from the reservoir. The reasons for this will be discussed further in section 6.3.

Based on filling rates for the past 5.0 million years, it is estimated that if injection were continued at the same rate, oil saturation would reach 55 percent in all areas of the lens by 6.0 million years. Therefore, under the assumed conditions, this reservoir would require approximately 5.0 million years to fill with oil.

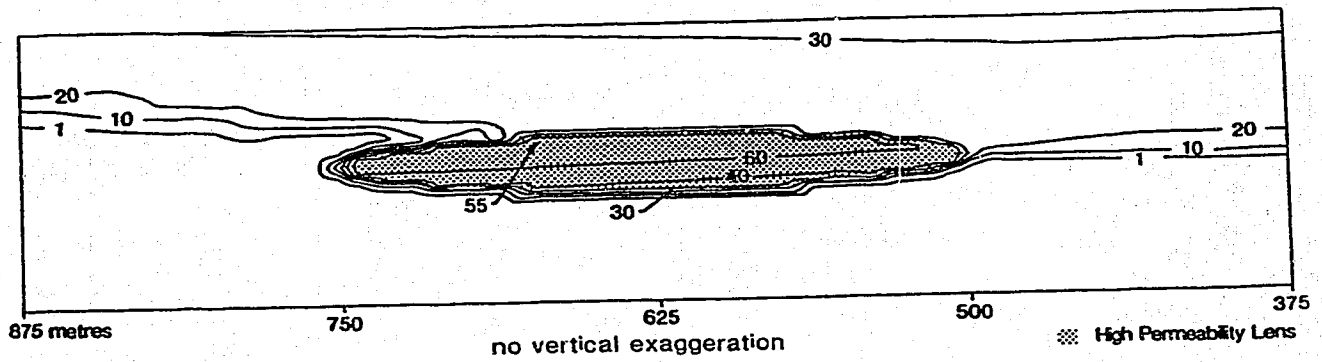


Figure 6.2: Detail of lens-area oil-saturation distribution at 5 000 000 years, Case Two. Contours in percent oil saturation.

6.2 Water Hydraulic Head

The steady state, water hydraulic-head distribution for Case Two is exactly the same as for Case One because the same water density and initial conditions were used in both cases. Figure 5.3 illustrates this pattern, of which a detailed explanation has been given in section 5.2.

The evolution of the water hydraulic-head surface during part two of the simulation is shown in Figure 6.3.

At the start of oil injection, the maximum value of water hydraulic head in the system increases, similar to that observed in Case One, because of the extra energy added to the system from fluid injection.

Overall, the hydraulic head patterns show two effects of increased oil saturation within the flow domain. First, the contours outlining the lens area are asymmetrical. This is caused by increased oil saturation in the top portion of the grid and within the lens (at later times), altering the direction of fluid-flow, and hence the fluid-potential pattern. Second, a visible difference exists between the shape of the hydraulic head contours upstream and downstream of the lens. The hydraulic head contours downstream of the lens are almost vertical. Upstream, the contours are not vertical. This illustrates the variable sensitivity of the hydraulic head pattern to changes in oil saturation.

The variable effect upstream/downstream of the lens can be explained by changes in oil saturation distribution. In both cases, there is a vertical in oil saturation gradient

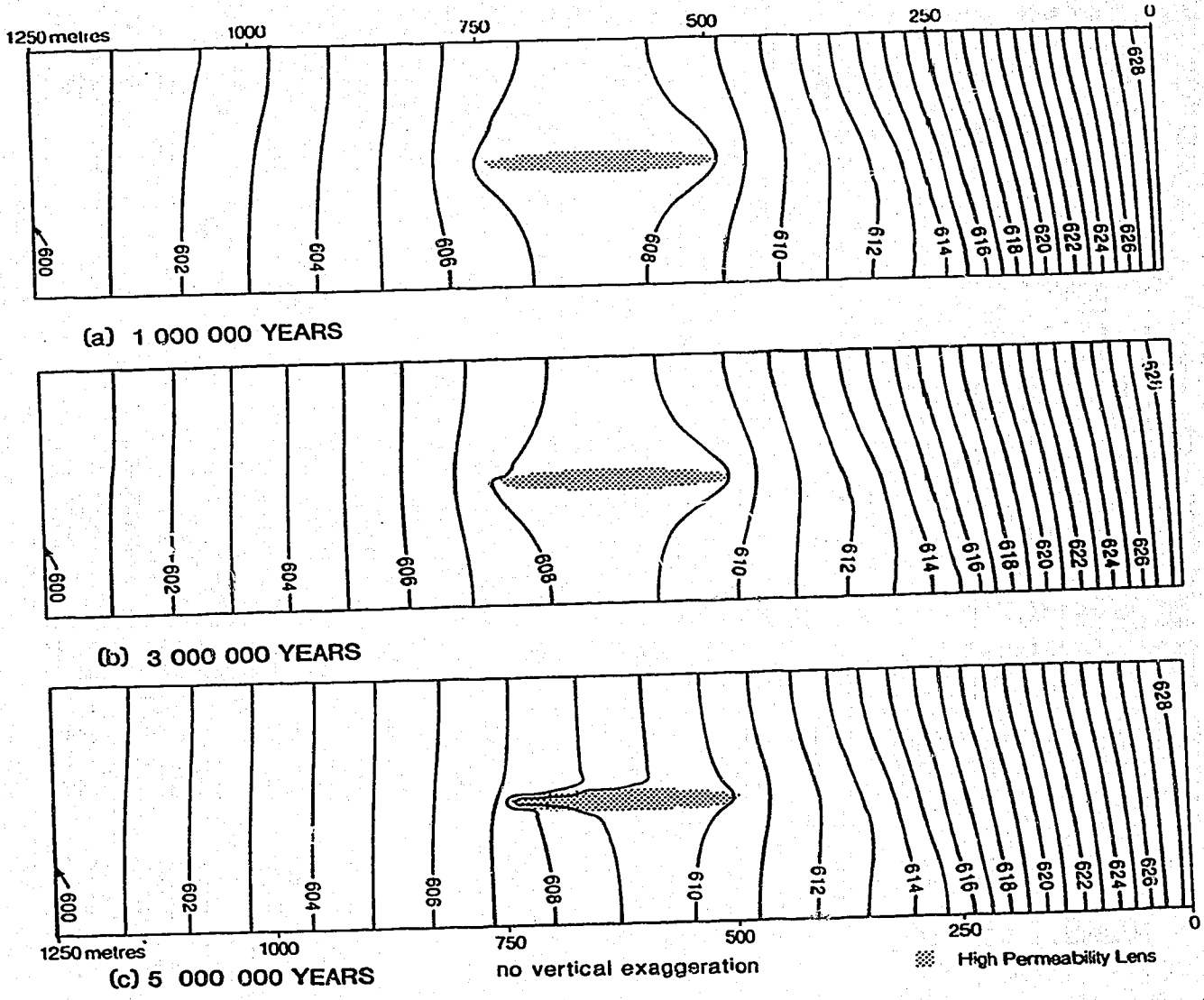


Figure 6.3: Water hydraulic-head distribution, Case Two. One metre contour interval.

across the flow domain. Upstream, the saturation varies from approximately 27 to 35 percent (bottom to top), which causes non-vertical hydraulic head contours. Downstream, the saturation varies from 0 to 30 percent, with no noticeable effect on the hydraulic head distribution. Therefore, subtle changes in saturation may or may not cause changes in the water fluid-potential patterns, depending on the position on the relative permeability curves where these changes take place.

The position of the transition zone is difficult to predict from these water potentiometric surfaces. The extent of the hydrocarbon saturated portion of the flow domain is hinted at by a slight bunching of the contours at the upstream end of the flow domain. It is interesting to note that the presence of oil shifts the contour values only 2.5 metres, a shift that could well be mistaken for the effect of another highly-permeable but non-saturated body nearby.

At 3.0 million years (Figure 6.3b) a small portion of the lens has reached 49 percent oil saturation, reducing the relative permeability to water in this area to near zero. Water is now being forced to flow around this area, which is reflected in the shape of the 608 metre contour. This effect is localized, and not noticeable elsewhere.

At 5.0 million years, the top 5.0 metres of the lens has reached 55 percent oil saturation, hence zero permeability to water. Water is starting to flow around that part of the lens. This effect is visible on the hydraulic head pattern in

Figure 6.3c. The iso-potential contours (608 to 610 metres) have begun to encircle the top 5.0 metres of the lens. This is the beginning of the isolation of that particular low permeability region from the rest of the flow domain. If the entire reservoir had reached zero relative permeability to water, it would be encircled by closed region of high fluid-potential, causing migrating water particles to flow around it, similar to the situation that existed after 2.0 million years in Case One.

In Case Two, asymmetrical water flow into, and around, the lens is indicated. This occurs because the relative permeability to water has not been reached zero throughout the lens. The non-uniform decrease in permeability has caused an asymmetrical fluid-flow pattern which is reflected in the shape of the hydraulic head contours in the lens area.

6.3 Oil Hydraulic Head

The distribution of oil hydraulic head at steady state is shown in Figure 6.4a, and in detail in Figure 6.4b. Hydraulic heads are higher than in Case One. This is due to a difference in oil density between the two cases, which can be explained by the comparison of two hypothetical fluids A and B. Applying equation 2.3 to A and B (where A is less dense than B) will result in higher hydraulic heads for fluid A, at the same point of measurement. This calculation, which illustrates the difference between hydraulic head values in cases one and two is contained in Appendix 4. It contains a

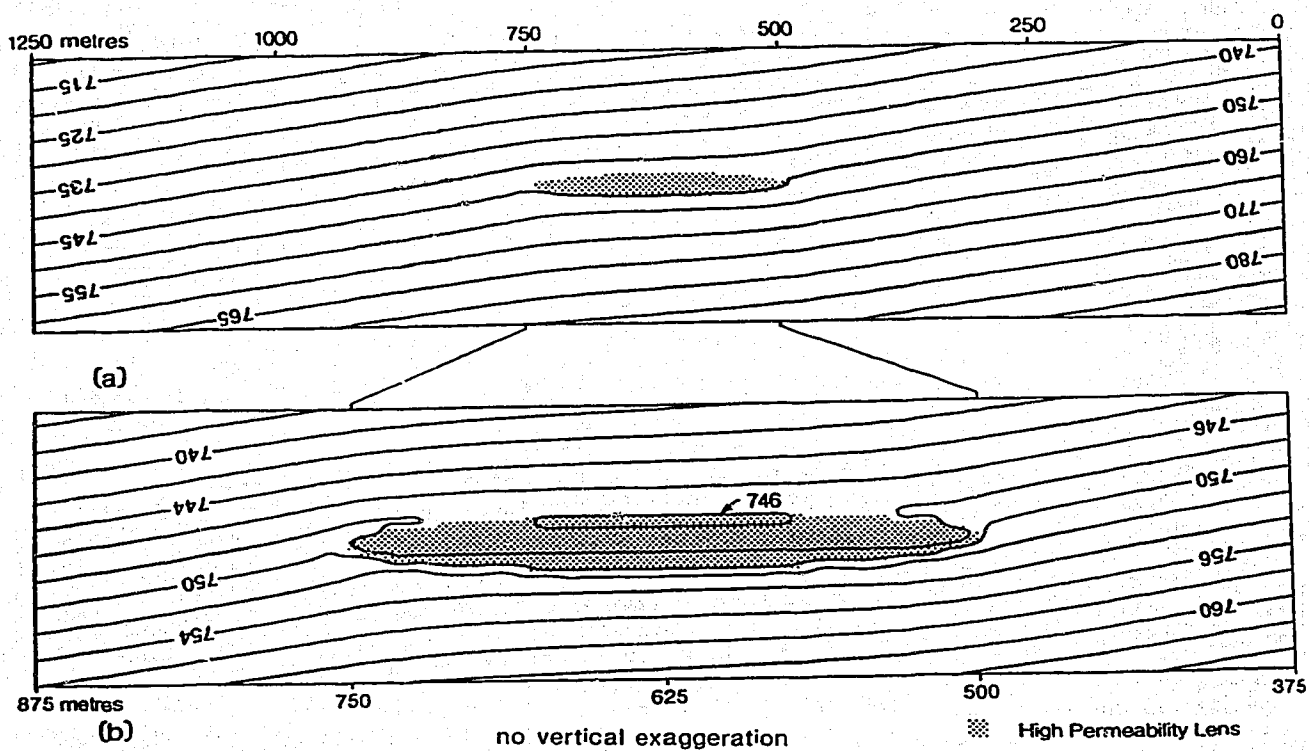


Figure 6.4: Oil hydraulic-head distribution, Steady State conditions, Case Two.
 (a) Five metre contour interval
 (b) Lens-area detail. Two metre contour interval.

sample calculation of an oil hydraulic-head value from a given water hydraulic head at a point near the upstream boundary of the flow domain.

The oil hydraulic-head pattern (Figure 6.4) is made up of three separate, but inter-related effects, namely: (1) buoyancy; (2) a highly-permeable lens; and (3) capillary pressures.

The buoyancy effect is clearly visible outside the lens area in Figure 6.4a. The tilted iso-potential contours are a result of the ~~vector summation~~ vector summation of the two separate driving forces on the fluid particles. For oil, in a hydrostatic environment, the driving force vector is vertical. For water, in a hydrodynamic environment the driving force vector is horizontal. The vector summation of these two forces yield the driving force vector for oil in a dynamic environment, namely that seen outside the lens area in Figure 6.4a. The iso-potentials resulting from a combination of lighter oil and flowing water are termed the buoyancy effect.

The highly-permeable lens effect, cannot be isolated from figures 6.4a or 6.4b, due to the insufficient resolving power of the 5.0 and 2.0 metre contour intervals. This effect arises because the permeability contrast between lens and matrix causes flow to focus into the upstream, and out the downstream, ends of an elliptical, highly-permeable rock body (Tóth and Rakhit, 1988). From results obtained in Case One (identical lens properties), the highly-permeable lens effect generates a maximum of \pm 2.4 metres difference in hydraulic

head, at the downstream and upstream ends of the lens, respectively.

The capillary pressure effect arises from differences in the capillary pressure curves at 100 percent water saturation. This effect acts normal to the lens boundary. Its magnitude can be calculated as the difference in the capillary pressures (at 100 percent water saturation) in the lens and matrix. In this instance, the magnitude equals 25.0 kPa or 3.0 metres of hydraulic head. This effect acts across the lens boundary and is directed inwards, from the matrix to the lens.

In Case Two, the summation of the buoyancy, highly-permeable lens, and capillary pressure effects does not produce a symmetrical, closed potentiometric-low, such as that seen in Case One.

Figure 6.5 is a schematic breakdown of the forces acting in the lens area. This figure is an interpretation of the simulated hydraulic-head distribution (Figure 6.4a). Six areas of interest are shown, numbered clockwise from the upper, upstream "corner" of the lens.

At steady state, oil flows into the lens from all directions. The resultants of the three force components are all directed inwards, although each vector has a different magnitude. At position 1, the capillary and permeability components override the buoyancy component. Oil flow is downstream (with respect to water) and downwards into the reservoir. At position 2, all three components are directed

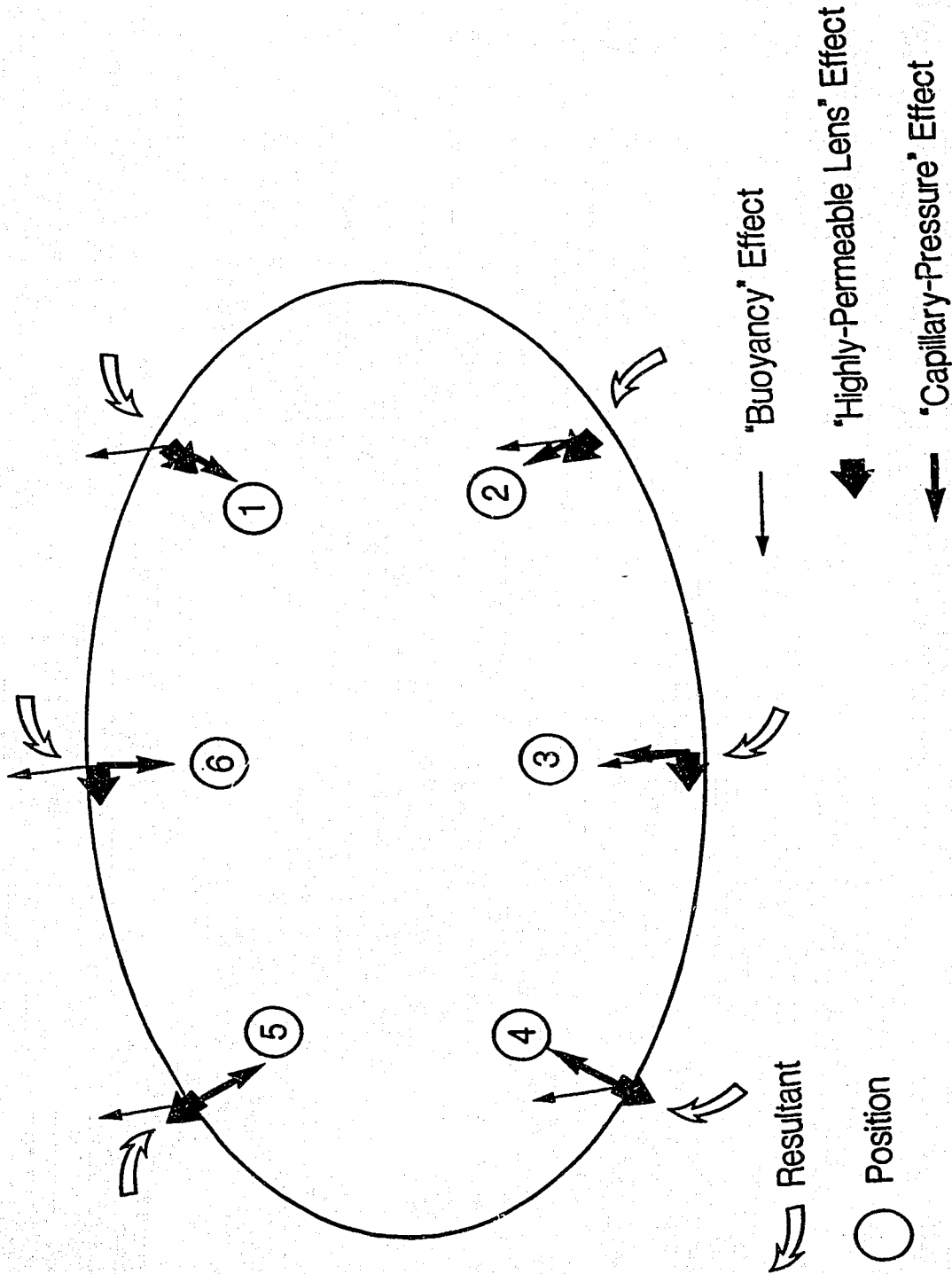


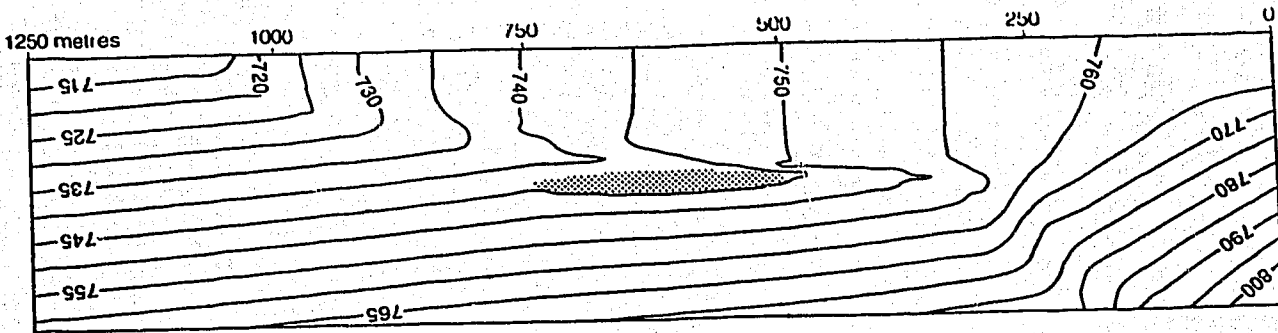
Figure 6.5: Schematic of forces acting in the area of the lens at steady state conditions.

in towards the lens, creating the most favorable position for oil entry. At position 3, the capillary and buoyancy components combine to direct flow upwards into the lens. At position 4, the resulting oil flow is upwards into the reservoir, but upstream with respect to water. The capillary force and buoyancy components combine to control the oil flow direction. At position 5, the net result is similar to position 4, but is weaker because only the capillary force component acts to draw oil into the lens. This would be the most likely position for oil to exit from the lens. At position 6, the resultant is directed downwards because the capillary force component is larger than the buoyancy force component.

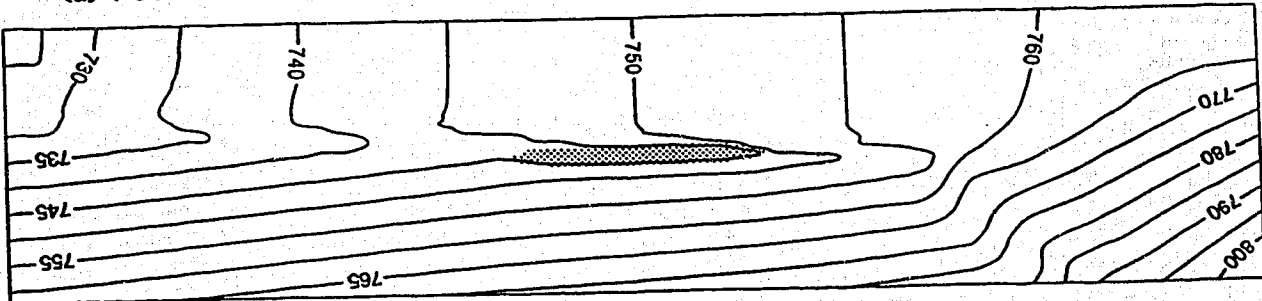
Figures 6.4 and 6.5 illustrate that oil entrapment in the reservoir is controlled by a complex super-position of buoyancy, permeability, and capillary derived forces.

The spatial and temporal evolution of the oil hydraulic-head surface during part two is shown in Figure 6.6. Details of the lens area at 1.0 and 5.0 million years are shown in figures 6.7a and 6.7b, respectively.

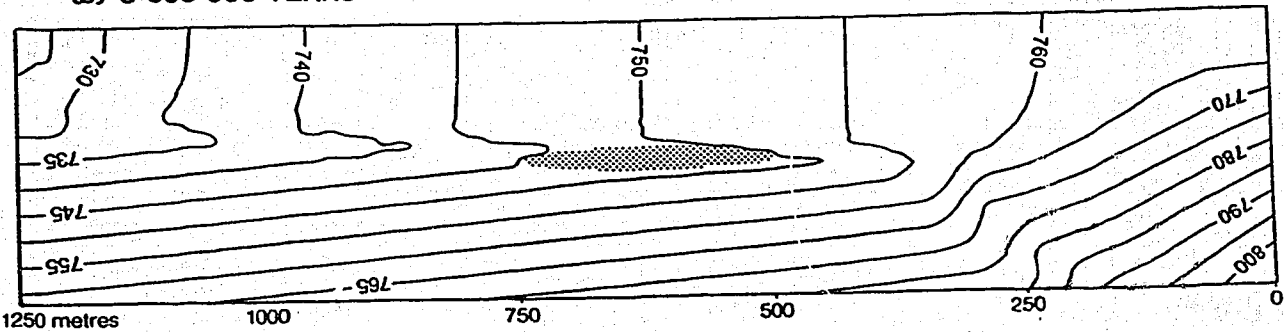
Outside the lens area, little change takes place in the hydraulic head surface during the 5.0 million year injection period. Upstream of the lens, oil flows upwards and downstream, as evidenced by the tilted contours in that region. Above the lens, oil flows horizontally downstream, as indicated by the near-vertical contour lines.



(a) 1 000 000 YEARS



(b) 3 000 000 YEARS



(c) 5 000 000 YEARS

no vertical exaggeration

High Permeability Lens

Figure 6.6: Oil hydraulic-head distribution, Case Two. Five metre contour interval.

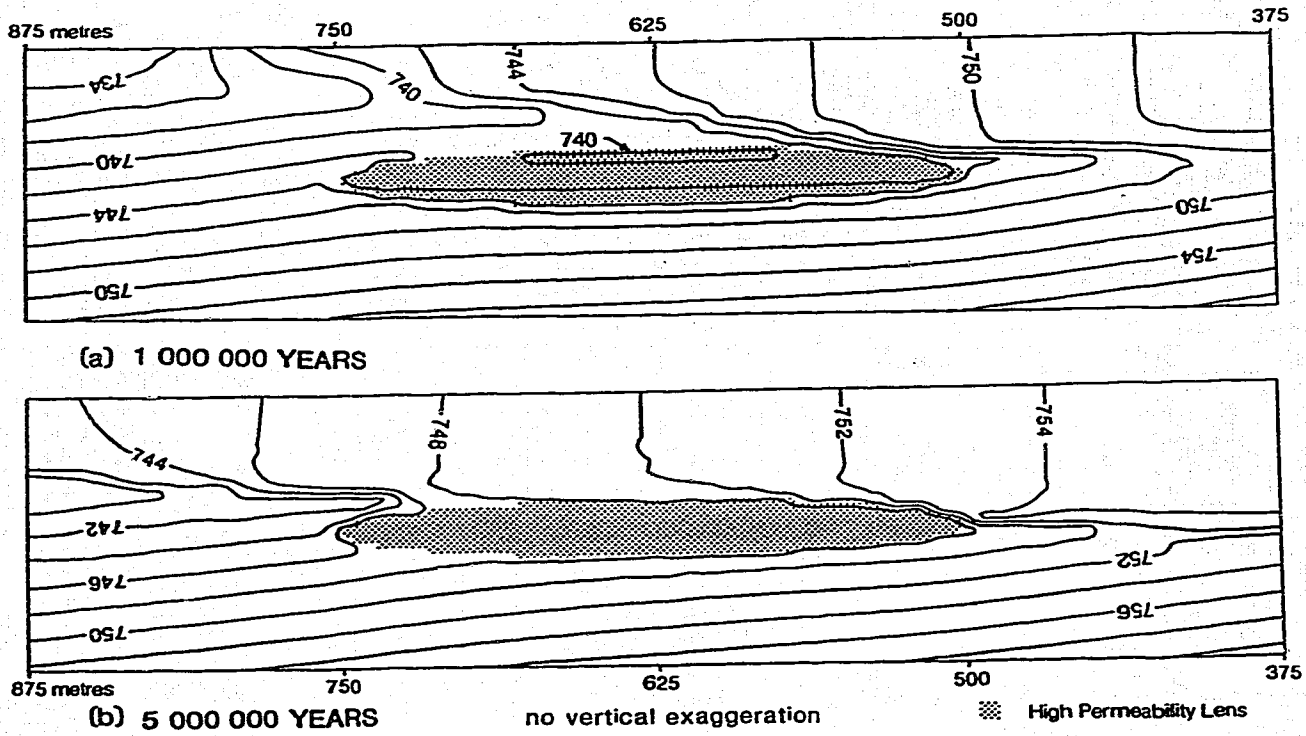


Figure 6.7: Lens-area detail of the oil hydraulic-head distribution, Case Two. Two metre contour interval.

Inside the lens, changes in the hydraulic head distribution take place as the lens fills with oil. At 1.0 million years (figures 6.6a and 6.7a) the pattern is similar to that at steady state. Oil is not yet entering the lens, but soon will be entering along the upper, upstream "corner" of the lens.

As oil fills the lens, the magnitude of the capillary pressure barrier changes. For example, by 2.0 million years (not illustrated) the capillary barrier will have been reduced from 3.0 to 1.4 metre of head. By the time 3.0 million years have elapsed, a portion of the lens has reached 50 percent oil saturation which is the point where capillary pressures are equal in the oil saturated lens and non-saturated matrix. This means that oil can leave the lens. This is visible in Figure 6.6b, where the 745 metre contour almost circles the entire reservoir, except for a small break at the "corner" of the lens (position 5 on Figure 6.5). Oil exits at a very slow rate into the low permeability unit. There is still a positive net flow of oil into the reservoir.

As time passes, the fully saturated portion of the reservoir grows in size. Associated with this is the loss of the reservoir's ability to trap oil.

The final hydraulic-head pattern is shown in Figure 6.6c and in detail in Figure 6.7b. On the regional scale there are distortions in the fluid-potential field but there is no direct indication of the presence of a lens. This is partly due to the use of a 5.0 metre contour interval, and partly as

a result of lens filling causing decreased disturbance to the flow field.

The lens is now leaking from the upper, and upper-downstream boundaries (positions 5 and 6, Figure 6.5). Now, only a very minor, inward component of flow is indicated by the potentiometric surface. Oil is still focused into the lens but not nearly as strongly as before.

It is hypothesized that if injection were continued to the eventual saturation of the lens, by 6.0 million years the lens would be indistinguishable from the rest of the flow domain (based exclusively on the oil hydraulic-head distribution). Any further advancement in time would most likely produce oil hydraulic-head distributions similar to Figure 6.6c. After this time, the oil hydraulic-head pattern would likely remain unchanged.

7.0 DISCUSSION

7.1 Sensitivity Analysis

Typically, in a numerical simulation study such as this, the sensitivity of the results to changes in input parameters would be investigated. Such an analysis would normally be conducted by altering an input parameter, re-running the simulation, and comparing the results with the original case. This type of quantitative analysis was not possible in this study due to the large number of input parameters, and the length of time required to run each simulation. Instead, a qualitative discussion of the sensitivity of the results will be presented, based on simulations conducted, but not included here.

As mentioned previously, SWANFLOW-2D assumes constant values of fluid viscosity and density, that is, they are not allowed to vary as a function of pressure. The largest and smallest pressure values encountered at any time, in any position, in either case, were 9181 and 5916 kPa. These values occurred in Case Two, during the oil injection part, in the lower-upstream, and upper-downstream corners, respectively, of the grid. Tables 7.1 and 7.2 illustrate the oil viscosity and density variations over these pressures, which were obtained from PVT curves for Belly River Formation oil samples (figures 4.8 and 4.9). It can be seen that the total change in the parameters over this (maximum) pressure range, is small (1.9 and 3.9 percent for density and

Table 7.1

Oil viscosity variation over the range of pressures encountered in the simulations.

Well	Viscosity @ Pmin (mPa·s) (5916 kPa)	Viscosity @ Pmax (mPa·s) (9181 kPa)
03-34-45-06 W6	1.15	1.04
10-34-45-06 W6	0.80	0.625
16-14-45-07 W6	0.625	0.74
14-17-45-07 W6	0.88	0.74
average	0.864	0.786
range	0.078	
percent variation	$0.078/2.0 \cdot 100 = 3.9 \%$	

source : AERCB Pressure-Volume-Temperature (PVT) data file.

Table 7.2

Oil density variation over the range of pressures encountered in the simulations.

Well	Density @ Pmin (kg/m ³) (5916 kPa)	Density @ Pmax (kg/m ³) (9181 kPa)
03-34-45-06 W6	763	750
10-34-45-06 W6	730	710
16-14-45-07 W6	712	688
14-17-45-07 W6	738	731
average	735.8	719.8
range		16
percent variation	$16/850 \cdot 100 = 1.9 \%$	

source : AERCB Pressure-Volume-Temperature (PVT) data file.

viscosity, respectively) in comparison to the magnitude of the data values. In the strictest sense, these variations should be accounted for, but in this case, the additional computing time required to obtain more accurate results is not warranted.

The input data can be divided into three groups, based on their sensitivity: (1) data that control the operation of the simulation; (2) data that, when changed, have a minor effect on the outcome of the simulation; and (3) data that, when changed, have a major effect on the outcome of the simulation.

The first group are the simulation control parameters. Their effect(s) do not directly affect the outcome of the simulations. These were discussed in section 4.5.

The second group are defined as those data which have only a minor effect on the outcome of the simulations, relative to the data in group three that have a major effect on the simulations. Data in the second group include: grid and lens size/shape; number/shape of grid blocks; magnitude and ratio of fluid viscosities; ratio of fluid densities; magnitude and ratio of permeabilities; magnitude and ratio of porosities; oil injection rate; and gradient/magnitude of water fluid-potentials. Each of these data, if altered enough, could have a major, if not controlling, effect on the simulation results. However, the simulation results are not as sensitive to changes in the group two data as compared to the group three data. By increasing/decreasing one or more of

these parameters, the results will be altered, but the alteration of the results is proportional to the change(s) made. For example, a small increase in the size of the lens will cause: slightly larger fluid-potential distortions; require the use of a larger grid; and lengthen the time required to fill the lens. The fluid-potential pattern will be of similar shape, and the lens will eventually fill with oil as before, but with a slightly longer filling time.

The third group include: fluid density; relative permeability curves; and capillary pressure curves. The simulation results were sensitive to small changes in these data.

The effect of changes in density on the simulation results become evident by comparison of cases one and two. The entire oil saturation distribution, and oil/water potentiometric surfaces are affected by a change in the fluid density. Furthermore, the oil flow direction outside the area of the lens is a function of the density difference between the fluids.

The critical parts of the relative permeability curves are their respective endpoint values, S_{oi} , and S_{wi} . These values control: the amount of residual oil left behind the front; the maximum attainable level of oil saturation; the minimum oil saturation required for oil flow; the ultimate oil recovery; and a number of other parameters. The shape of the curves themselves control the rate at which permeability to each fluid is affected by changes in saturation.

Simulation results are also very sensitive to changes in capillary pressure curves, which are critical as far as trapping of oil is concerned. Each of the three parts of the curve are important, namely: (1) the entry pressure ($@S_w = 100\%$), to which the trapping capacity of the reservoir is directly related; (2) the shape of the middle part of the curve, which influences how rapidly changes in capillary pressures occur with changes in saturation; and (3) the shape of the "tail" ($S_w \cong S_{wi}$) portion of the curve which is related to S_{wi} , and the maximum attainable oil saturation.

It should be noted that laboratory-derived capillary pressure curves may not represent long term reservoir conditions. That is, that over a long period of time the wettability factors which control the shape of the capillary pressure curves may change. This could cause changes in the shape of the capillary pressure curve(s), which would cause the real conditions to differ from the simulated conditions.

The same long-term effect could alter the relative permeability curves. The possibility exists that, for example, the irreducible oil saturation may eventually reach zero. That is, long-term wettability changes or water washing could allow all of the oil to be removed from the pore space. This could explain why no traces (or "trails") of oil exist in carrier beds along known migration pathways.

These long term changes could be simulated by altering the relative-permeability and capillary-pressure curves at certain times during the simulation, but this would only

serve to further complicate the fluid-potential patterns that are evolving as the simulation proceeds. For the purpose of this work, long term changes in the input data did not warrant investigation.

7.2 Effect of Oil on Potentiometric Surfaces

One of the original objectives was to study the oil and water potentiometric surfaces during oil emplacement, with emphasis on the degree and distribution of hydrocarbon saturation. Results presented here (figures 5.1 - 5.8, 6.1 - 6.4, 6.6 - 6.7), illustrate these effects. In general, the following are found:

- (1) the water potentiometric surface in an oil-free environment is a function of the regional fluid-potential gradient, permeability contrast, lens geometry, and lens orientation relative to the regional fluid-flow direction.
- (2) the oil potentiometric surface in an oil-free environment is a function of the water potentiometric surface, but is modified by the capillary pressure curves of the particular rock unit, and the density difference between oil and water.
- (3) once oil is introduced into the system, both fluid-potential patterns begin to change, as a result of the functional relationship between oil saturation and permeability (relative permeability curves), and oil saturation and pressure (capillary pressure curves).
- (4) the original, localized potentiometric low in the lens area is reduced as the lens fills with oil. As the lens

fills, its ability to trap oil is reduced. Eventually, once full, the oil potentiometric surface appears similar to the water potentiometric surface at steady state (with modifications for capillary pressures).

(5) for the water potentiometric surface, as emplacement and concentration progress, the relative permeability to water decreases. This is manifested in an alteration of, and eventually the destruction, of the fluid-potential anomaly.

(6) for intermediate cases, i.e., partially full lenses, the potentiometric surfaces for either fluid are difficult to interpret in terms of degree and distribution of oil saturation. That is, it is difficult to take a potentiometric surface from a flow domain containing partially filled lenses, and predict the degree and extent of the oil saturation. This is because too many variables combine to produce the fluid-potential surfaces. The solution of the inverse problem: from potentiometric surface to geology, is non-unique. Oil saturation cannot be determined with any degree of certainty, given only the water potentiometric surface.

7.3 Implications for Exploration

Previous work (Rakhit, 1987; Tóth and Rakhit, 1988) has illustrated that reservoir-quality rock bodies cause characteristic perturbations of the water potentiometric surface. The present study extends their analysis by including an oil phase in the flow domain. It illustrates the

genetic relationship between lens, oil accumulation, and fluid-potential anomalies.

Earlier works have shown how Hubbert's UVZ method and single-phase potentiometric surface analysis can be useful for oil exploration (Dahlberg, 1982; Tóth and Rakhit, 1988). The present study investigates these methods further by accounting for oil in the reservoir, and the resulting reduction in permeability to water. It also accounts for the presence of oil, and includes capillary pressures in the flow domain.

The single-phase potentiometric-surface technique is hampered by the fact that, water potential surfaces are affected by the presence of oil. It is impossible, therefore, to differentiate between water-potential anomalies generated by low relative permeability to water or by low intrinsic permeability.

Figure 7.1 illustrates the proposed "iterative improvement process" that could be used for this problem. First, the geology of a flow domain is assumed, using where possible, information from other sources (geophysics, well logs). Next, the data are input into the numerical model, and a numerical UVZ analysis completed (such as shown in any of the oil/water hydraulic head figures). The simulated potentiometric surface can then be compared to the field-derived water potentiometric-surface. In this manner, various geological alternatives, and their resulting fluid-potential patterns can be generated and compared, in order to try and

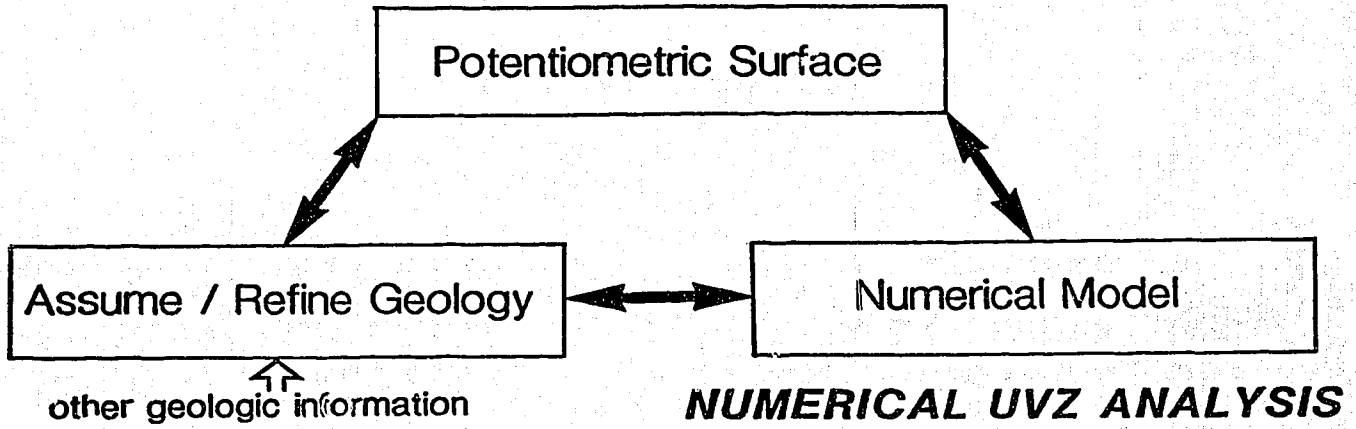


Figure 7.1: Schematic of the proposed "iterative improvement process".

determine the geology and the degree and distribution of hydrocarbon saturation, i.e., whether an oil filled lens is present or not.

8.0 CONCLUSIONS

Numerical modelling has, in general, shown that:

- 1) It is possible to simulate secondary oil migration and entrapment in a lenticular reservoir, on a basinal scale, using currently (1989) existing software and computer hardware.
- 2) Fluid-potential fields of water and oil govern fluid flow directions, which are modified by:
 - (i) highly-permeable lenses, situated within the flow field;
 - (ii) buoyancy;
 - (iii) capillary pressures.
- 3) The distribution of fluid-potentials is genetically related to relative permeability and capillary pressure curve properties which are, in turn, functions of oil saturation distribution. As migration proceeds, oil saturation distribution, thus fluid-potential distributions, change in time and space.
- 4) Entrapment of oil within a reservoir is controlled by fluid-potential conditions that are generated by regional fluid-potential gradients, and modified by super-position of the highly-permeable lens, buoyancy, and capillary pressure effects.
- 5) In certain cases, fluid flow is dominated by one or more of these effects. This can lead to opposing fluid flow directions.

6) Capillary pressures and relative permeabilities, which have not been taken into account in previous works, play a major, if not controlling, role in the migration and entrapment of oil in lenticular reservoirs.

Specific conclusions from the results fall into three categories, dealing with: oil migration and entrapment; potentiometric surface effects; and implications for oil exploration techniques.

Oil migration

- Medium gravity oil (850 kg/m^3) will tend to migrate in the carrier bed along the upper boundary with a less permeable rock. Under this condition, lenticular reservoirs can be charged with oil moving downward from above.
- Once a reservoir is filled with oil, it will remain so, even after the supply of oil is terminated. This is a direct result of fluid-potential and permeability relationships within the reservoir. Oil will remain trapped until fluid-potential conditions in the reservoir change (possibly through long term changes in the capillary pressure or relative permeability curves).

Fluid-potential effects

- Water-filled lenticular reservoirs are favorable sites for oil accumulations owing to favorable permeability and capillary pressure conditions. These reservoirs generate characteristic fluid-potential patterns.

- Oil preferentially enters and accumulates within a reservoir until the oil saturation level alters the fluid-potential conditions such that oil may exit. This happens through changes in relative permeability (to oil and water), and changes in capillary pressures inside and outside the reservoir.
- The reduction in relative permeability to water, as a result of increased oil saturation within a lens, can modify and even reverse, the highly-permeable lens effect.
- Since capillary pressure and relative permeability curves are strongly non-linear, the effects on fluid-potential conditions are highly sensitive to changes in saturation at certain saturation levels.

Oil exploration techniques

- It is difficult (if not impossible) in some cases, using the water potentiometric surface, to distinguish between an oil-saturated reservoir with high intrinsic permeability and a water-filled lens of low permeability. In these cases, it is mandatory to use other information, including: oil potentiometric surfaces; and other geological, geophysical, and chemical information in the exploration effort.
- Oil hydraulic-head surfaces, as shown, are analogous to Hubbert's U surface, accounting for capillary forces and the presence of oil.
- Numerically calculated oil potentiometric-surfaces (such as shown) are more accurate, more widely applicable, and easier

to calculate than Hubbert's U surface. As such, the numerical simulations presented here demonstrate the operation of the numerical UVZ method.

9.0 REFERENCES

Abriola, L.M. and G.F. Pinder, 1985a, A Multiphase Approach to the Modeling of Porous Media Contamination by Organic Compounds, 1. Equation Development: Water Resources Research, v. 21, no. 1, p. 11-18.

Abriola, L.M. and G.F. Pinder, 1985b, A Multiphase Approach to the Modeling of Porous Media Contamination by Organic Compounds, 2. Numerical Simulation: Water Resources Research, v. 21, no. 1, p. 19-36.

AERCB (Alberta Energy Resources Conservation Board), Pressure-Volume-Temperature Files, and Special Core Analysis Files, Records Centre, Calgary, Alberta, Canada.

AGAT Laboratories, (Undated), Table of Formations of Alberta, Calgary, Alberta, Canada.

Arthur D. Little, Inc., 1983, S-Area Two Phase Flow Model, technical report for Wald, Harkrader & Ross, Washington, D.C.

Berg, R.R., 1975, Capillary Pressures in Stratigraphic Traps: AAPG Bulletin, v. 59, no. 6, p. 939-956.

Craig, Jr., F.F., 1971, The Reservoir Engineering Aspects of Waterflooding: Society of Petroleum Engineers, Monograph 5, Dallas, Texas, USA, 141 p.

Creaney, S., and J. Allan, 1988 in press, Hydrocarbon Generation and Migration in the Western Canada Sedimentary Basin: Proceedings of the Geological Society of London, 37 p.

Dahlberg, E.C., 1982, Applied Hydrodynamics in Petroleum Exploration: New York, Springer-Verlag, 161 p.

Davis, R.W., 1987, Analysis of Hydrodynamic Factors in Petroleum Migration and Entrapment: AAPG Bulletin, v. 71, no. 6, p. 643-649.

Dullien, F.A.L., 1979, Porous Media, Fluid Transport and Structure: Academic Press, 396 p.

Durand, B., Ph. Ungerer, A. Chiarelli, J.L. Oudin, 1983, Modelling of Oil Migration. Application to Two Examples of Sedimentary Basins (English Translation of: Modelisation de la Migration de l'Huile Application a Deux Exemples de Bassins Sedimentaires): proceedings, 11th World Petroleum Congress, London, p. 3-15.

- England, W.A., A.S. Mackenzie, D.M. Mann, and T.M. Quigley, 1987, The Movement and Entrapment of Petroleum Fluids in the Subsurface: Journal of the Geological Society, London, v. 144, p. 327-347.
- Faust, C.R., 1985, Transport of Immiscible Fluids Within and Below the Unsaturated Zone: A Numerical Model: Water Resources Research, v. 21, no. 4, p. 587-596.
- _____, and J.O. Rumbaugh III, 1986, SWANFLOW-2D: Simultaneous Water, Air, and Nonaqueous Phase Flow Model in Two Dimensions, User Documentation, Version 1.0: Geotrans Inc., Herndon, Virginia, 69 p.
- Franchi, J.R., K.J. Harpoole, and S.W. Bujnowski, 1982, BOAST: A Three-Dimensional, Three-Phase, Black Oil Applied Simulation Tool (Version 1.1), Volume 1, Technical Description and FORTRAN Code: United States Department of Energy, Bartlesville, Oklahoma, USA, 180 p.
- Freeze, R.A., and J.A. Cherry, 1979, Groundwater: Englewood Cliffs, N. J., Prentice-Hall, 604 p.
- Garven, G., 1989, A Hydrogeologic Model for the Formation of the Giant Oil Sands Deposits of the Western Canada Sedimentary Basin: American Journal of Science, vol. 289, no. 2, p. 105-166.
- Hubbert, M.K., 1940, The Theory of Ground-Water Motion: Journal of Geology, v. 48, no. 8, p. 785-944.
- _____, 1953, Entrapment of Petroleum Under Hydrodynamic Conditions: AAPG Bulletin, v. 37, no. 8, p. 1954-2026.
- Hunter, D.E., 1966, An Investigation on the Waterflooding Behaviour of Preserved Cores from the Belly River Formation - Pembina Field: Imperial Oil Limited, Producing Department - Western Region, Laboratory Report No. L-38166, Production Research and Technical Service Department, Calgary, Alberta, June 1966, 60 p.
- Huyakorn, P.S., and G.F. Pinder, 1983, Computational Methods in Subsurface Flow: Academic Press, Orlando, Florida, 473 p.
- Iwuagwu, C.J., and J.F. Lerbekmo, 1982, The Petrology of the Basal Belly River Sandstone Reservoir, Pembina Field, Alberta: Bulletin of Canadian Petroleum Geology, vol. 30, no. 3, p. 187-207.

- _____, and _____, 1984, Application of Outcrop Information to Subsurface Exploration for Sandstone Reservoirs; Basal Belly River Formation (Upper Cretaceous), Alberta Foothills: The Mesozoic of Middle North America, D.F. Stott and D.J. Glass, Editors, Canadian Society of Petroleum Geologists Memoir 9, p. 387-400.
- Jabour, H., and K. Nakayama, 1988, Basin Modeling of Tadia Basin, Morocco, for Hydrocarbon Potential: AAPG Bulletin, v. 72, no. 9, p. 1059-1073.
- Jennings, J.B., 1987, Capillary Pressure Techniques: Application to Exploration and Development Geology: AAPG Bulletin, v. 71, no. 10, p. 1196-1209.
- Lerbekmo, J.F., 1963, Petrology of the Belly River Formation, Southern Alberta Foothills: Sedimentology, v. 2, p. 54-86.
- Mackenzie, A.S., and T.M. Quigley, 1988, Principles of Geochemical Prospect Appraisal: AAPG Bulletin, v. 72, no. 4, p. 399-415.
- McAuliffe, C.D., 1980, Oil and Gas Migration: Chemical and Physical Constraints: Problems of Petroleum Migration, AAPG Studies in Geology, No. 10, Edited by W.H. Roberts, III and R.J. Cordell, AAPG, Tulsa, Oklahoma, p. 89-107.
- McDonald, M.G., and A.W. Harbaugh, 1983, A Modular Three-Dimensional Finite-Difference Ground-Water Flow Model (MODFLOW): United States Geological Survey Open File Report, USGS Printing Office, Washington, D.C., 528 p.
- Nakayama, K., 1987, Hydrocarbon-Expulsion Model and Its Application to Niigata Area, Japan: AAPG Bulletin, v. 71, no 7, p. 810-821.
- _____, and I. Lerche, 1987a, Basin Analysis by Model Simulation: Effects of Geologic Parameters on 1-D and 2-D Fluid Flow Systems with Applications to an Oil Field: Gulf Coast Association of Geological Societies Transactions, v. 37, p. 175-184.
- _____, and _____, 1987b, Two-Dimensional Basin Analysis: Migration of Hydrocarbons in Sedimentary Basins, IFP Exploration Research Conference no. 45, edited by B. Doligez, Editions Technip, p. 597-611.
- North, F.K., 1985, Petroleum Geology: Allen and Unwin, Boston, 607 p.

- Obdam, A.N.M., and E.J.M. Veling, 1987, Elliptical Inhomogeneities in Groundwater Flow - An Analytical Description: *Journal of Hydrology*, v. 95, p. 87-96.
- Ogunyomi, O., and L.V. Hills, 1977, Depositional Environments, Foremost Formation (Late Cretaceous), Milk River Area, Southern Alberta: *Bulletin of Canadian Petroleum Geology*, v. 25, no. 5, p. 929-968.
- Osborne, M., and J. Sykes, 1986, Numerical Modeling of Immiscible Organic Transport at the Hyde Park Landfill: *Water Resources Research*, v. 22, no. 1, p. 25-33.
- Parks, K., and J. Tóth, 1988, Relations Between Fluid-Potential Anomalies, Sand Lenses and Oil Deposits, Belly River Formation, near Buck Lake, Alberta, Canada; Ramifications for Exploration: *GSA Abstracts with Programs*, v. 20, no. 7, p. A260.
- Parks, K., 1989, Groundwater Flow, Pore-Pressure Anomalies and Petroleum Entrapment, Belly River Formation, West-Central Alberta: M.Sc. Thesis, University of Alberta, Edmonton, Alberta, 132 p.
- Peaceman, D.W., 1977, *Fundamentals of Numerical Reservoir Simulation*: Elsevier, New York, USA, 176 p.
- Pinder, G.F., and L.M. Abriola, 1986, On the Simulation of Nonaqueous Phase Organic Compounds in the Subsurface: *Water Resources Research*, v. 22, no. 9, p. 109S-119S.
- Podruski, J.A., J.E. Barclay, A.P. Hamblin, P.J. Lee, K.G. Osadetz, R.M. Procter, and G.C. Taylor, 1988, Conventional Oil Resources of Western Canada (Light and Medium), Part 1: Resource Endowment: *Geological Survey of Canada, Paper 87-26*, 149 p.
- Price, L.C., 1976, Aqueous Solubility of Petroleum as Applied to its Origin and Primary Migration: *AAPG Bulletin*, v. 57, no. 2, p. 213-244.
- Rakhit, K., 1987, Potentiometric Surface Anomalies Due to Flow Through Highly Permeable, Lenticular Clastic Rocks and Their Application in Petroleum Exploration: M.Sc. Thesis, University of Alberta, Edmonton, Alberta, 166 p.
- Sabry, H., 1988, Lithofacies, Depositional Environments and Reservoir Quality of the Basal Belly River Sands in South-Central Alberta, Canada: *CSPG Reservoir*, vol. 15, no. 1, p. 1-2.
- Sampson, R.J., 1978, SURFACE II Graphics System (Revision One): Series on Spatial Analysis, Number One, Kansas Geological Survey, Lawrence, Kansas, USA, 240 p.

- Shouldice, J.R., 1979, Nature and Potential of Belly River Gas Sand Traps and Reservoirs in Western Canada: Bulletin of Canadian Petroleum Geology, v. 27, no. 2, p. 229-241.
- Schowalter, T.T., 1979, Mechanics of Secondary Hydrocarbon Migration and Entrapment: AAPG Bulletin, v. 63, no. 5, p. 723-760.
- Streeter, V.L., and E.B. Wylie, 1981, Fluid Mechanics, First SI Metric Edition: McGraw-Hill Ryerson Ltd., 562 p.
- Tissot, B.P., and D.H. Welte, 1984, Petroleum Formation and Occurrence, Second Revised and Enlarged Edition: Springer-Verlag, Berlin, 699 p.
- _____, 1987, Migration of Hydrocarbons in Sedimentary Basins: A Geological, Geochemical and Historical Perspective: Migration of Hydrocarbons in Sedimentary Basins, IFP Exploration Research Conference no. 45, edited by B. Doligez, Editions Technip, p. 1-19.
- Tóth, J., 1962, A Theory of Groundwater Motion in Small Basins in Central Alberta, Canada: Jour. of Geophys. Research, v.67, no. 11, p. 4375-4387.
- _____, 1966, Groundwater Geology, Movement, Chemistry, and Resources Near Olds, Alberta: Research Council of Alberta Bulletin 17, 126 p.
- _____, 1970, Relation Between Electric Analogue Patterns of Groundwater Flow and Accumulation of Hydrocarbons: Canadian Journal of Earth Sciences, v. 7, no. 3, p. 988-1007.
- _____, 1986, Models of Subsurface Hydrology of Sedimentary Basins: Proceedings, Third Canadian/American Conference on Hydrogeology, edited by B. Hitchon, S. Bachu, and C.M. Sauveplane, published by National Water Well Association, p. 1-18.
- _____, and K. Rakhit, 1988, Exploration for Reservoir Quality Rock Bodies by Mapping and Simulation of Potentiometric Surface Anomalies: Bulletin of Canadian Petroleum Geology, v. 36, no. 4, p. 362-378.
- Ungerer, P., F. Bessis, P.Y. Chenet, B. Durand, E. Nogaret, A. Chiarelli, J.L. Oudin, and J.F. Perrin, 1984, Geological and Geochemical Models in Oil Migration; Principles and Practical Examples: AAPG Memoir 35, Petroleum Geochemistry and Basin Evaluation, edited by G. Demaison and R.J. Murriss, p. 53-77.

Ungerer, P., B. Doligez, P.Y. Chenet, J. Burrus, F. Bessis, E.L. Lafargue, C. Giroir, O. Heum, and S. Eggen, 1987, A 2-D Model of Basin Scale Petroleum Migration by Two-Phase Fluid-Flow. Application to Some Case Studies: Migration of Hydrocarbons in Sedimentary Basins, IFP Exploration Research Conference no. 45, edited by B. Doligez, Editions Technip, p. 415-456.

Vugrinovich, R., 1988, Relationships Between Regional Hydrogeology and Hydrocarbon Occurrences in Michigan, USA: Journal of Petroleum Geology, v. 11, no. 4, p. 429-442.

Wells, P.R.A., 1988, Hydrodynamic Trapping in the Cretaceous Nahr Umr Lower Sand of the North Area, Offshore Qatar: Journal of Petroleum Technology, v. 40, no. 3, p. 357-361.

Welte, D.H., and M.A. Yüklér, 1981, Petroleum Origin and Accumulation in Basin Evolution-A Quantitative Model: AAPG Bulletin, v. 65, no. 8, p. 1387-1396.

Williams, G.D., and C.F. Burk Jr., 1964, Upper Cretaceous: Chapter 12, Geological History of Western Canada, edited by R.G. McCrossan and R.P. Glaister, Alberta Society of Petroleum Geologists, p. 169-189.

Zawisa, L., 1986, Hydrodynamic Conditions of Hydrocarbon Accumulation Exemplified by the Carboniferous Formation in the Lublin Synclorium, Poland: SPE Formation Evaluation, v. 1, no. 2, p. 286-294.

Appendix 1**Results of waterflood tests on selected Belly River cores.**

Well	S _{wi}	S _{oi}	por.	air perm.	comments
06-16-48-3 W5	31.9	26.8	17.7	228.	
	35.6	24.4	18.0	78.	
	45.8	21.8	17.3	33.	
	40.6	23.1	18.8	29.	
	58.7	26.9	15.6	5.3	
	49.2	28.4	13.6	4.4	
	58.2	17.8	14.9	3.8	
16-35-47-6 W5	46.5	32.4	14.3	0.8	
	41.6	30.8	13.2	0.45	
	58.2	29.7	13.6	0.53	
	47.9	37.4	14.1	0.41	
	47.9	32.0	14.8	0.89	
	53.9	31.1	14.1	0.18	
06-03-48-5 W5	55.8	24.2	18.0	12.8	
	48.5	29.8	18.5	35.3	
	59.8	28.8	14.5	0.93	
	65.9	28.8	14.7	0.80	
04-25-47-4 W5	49.6	17.9	14.3	3.07	
	64.4	7.0	16.3	12.0	
	64.6	12.1	16.3	39.3	
	56.2	15.3	15.6	4.54	
	56.1	31.8	16.0	6.35	
10-12-47-4 W5	39.7	29.7	16.4	114.	
	40.0	29.5	17.2	176.	
	42.0	29.8	16.2	7.8	
	39.8	29.0	16.9	35.0	
	85.0		13.0	.38	C-P test
	85.0		14.9	.33	"
	85.0		15.2	.51	"
	80.0		15.0	1.30	"
	35.0		18.1	250.	"
	40.0		18.5	105.	"
	35.0		19.6	260.0	"
	55.0		17.0	8.6	"
	40.0		18.7	59.0	"
	85.0		15.3	0.53	"
	80.0		15.9	1.32	"
	80.0		15.5	0.75	"

Well	S _{wi}	S _{oi}	por.	air perm.	comments
02-13-47-4 W5	43.0	31.0	16.3	24.0	
	48.0	31.0	13.9	11.0	
	51.0	30.0	16.3	4.7	
	43.0	30.0	16.2	31.0	
	42.0	29.0	13.5	8.8	
	85.0		13.9	0.31	C-P test
	88.0		14.1	0.14	"
	83.0		14.3	0.90	"
	28.0		16.9	56.0	"
	77.0		15.2	2.3	"
	70.0		16.5	3.6	"
	63.0		17.6	2.5	"
	58.0		17.8	10.9	"
	65.0		15.6	3.9	"
	53.0		15.9	6.1	"
08-12-48-3 W5	25.3		21.1	215.	"
	31.9		20.1	90.	"
	31.1		20.1	73.	"
	33.4		18.4	34.	"
	51.1		15.8	1.8	"
10-23-48-6 W5	38.0	26.0		79.	
10-15-48-6 W5	50.0	22.0		15.	
10-23-48-6 W5	52.0	15.0		5.3	
14-08-49-9 W5	30.0	42.0		1.41	
14-17-49-9 W5	32.0	28.0		256.	
	32.0	26.0		51.5	
14-34-47-2 W5	40.8	14.3	22.2	148.	
	46.8	13.8	19.6	60.	
	51.7	19.0	19.5	52.	
	55.4	19.4	18.2	23.	
	47.2	14.1	18.8	18.	
10-36-47-4 W5	39.0	17.9	21.0	379.	
	36.3	22.0	18.2	116.	
	45.3	24.8	18.0	68.	
	43.7	22.9	18.3	54.	
	46.0	23.5	18.0	27.	
	64.8	21.1	17.3	14.	
	56.7	19.7	15.0	5.8	
	55.5	24.7	16.0	2.6	

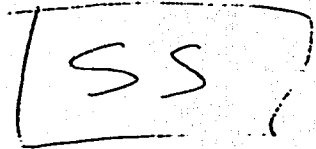
Well	S _{wi}	S _{oi}	por.	air perm.	comments
14-14-48-3 W5	52.8 62.8	21.3 20.4	19.0 16.2	92. 7.7	
Average	46.7	24.7	16.7	n/c	
Range	25.0 to 65.0	15.0 to 42.0	13.0 to 22.0	379. to 0.14	

Appendix 2

Sample Computer Output, Case One.

Listing of 3720UT at 02:52:52 on FEB 5, 1980 for CCID=BNR on UALTAMTS

Page 1



S W A M F L O W - 2 D

SIMULTANEOUS WATER, AIR, AND NAPL FLOW IN TWO DIMENSIONS

WRITTEN BY:

CHARLES R. FAUST
JAMES S. RUMSDEN

RESTRANS, INC.
250 EXCHANGE PLACE
SUITE A
HERNDON, VA

LENS 10:1 GRADIENT = 0.02 EPSILON = 1000 ----STEADY STATE----
DATE ---- 02 FEB 1980 RUN NO ---- 7_2

NUMBER OF BLOCKS IN THE X-DIRECTION (COLUMNS) = 50
NUMBER OF BLOCKS IN THE Z-DIRECTION (LAYERS) = 20
MAXIMUM OF NEWTON-RAPHSON ITERATIONS = 5
MAXIMUM SANDWICH = 0
MAXIMUM NUMBER OF TIME STEPS = 0
NUMBER OF ACTIVE GRID BLOCKS = 1740
NUMBER OF TIME STEPS BETWEEN PRINTOUTS = 50
PRINT NAPL AND WATER POTENTIALS? (1=YES) = 1
PRINT DETAILED KR TABLES? (1=YES) = 1
WRITE A PLOT FILE? (1=YES) = 0
NUMBER OF OBSERVATION BLOCKS = 0
WRITE A RESTART FILE? (1=YES) = 1

GRID BLOCK THICKNESS (DY) = 1.0000
MASS BALANCE TOLERANCE FOR NEWTON-RAPHSON IT. = 0.10000E-01
INITIAL TIME VALUE = 0.00000E+00
WATER DENSITY = 1000.0
NAPL DENSITY = 1000.0
WATER VISCOSITY = 0.10000E-02
NAPL VISCOSITY = 0.20000E-02
GRAVITATIONAL CONSTANT IN THE Z-DIRECTION = -9.8100
GRAVITATIONAL CONSTANT IN THE X-DIRECTION = 0.00000E+00

3 PC-KR TABLES WILL BE READ

***** TABLE NUMBER 1 *****

Table with 4 columns: NAPL-WATER CAP. PRESSURE, WATER SATURATION, RELATIVE PERM. WATER, RELATIVE PERM. NAPL. Rows 83-97.

AIR-NAPL SYSTEM -- PC-KR TABLE NUMBER 1
NAPL KR AT RESIDUAL WATER SATURATION : 0.68000

Table with 4 columns: AIR-NAPL CAP. PRESSURE, AIR SATURATION, RELATIVE PERM. NAPL, RELATIVE PERM. AIR. Rows 98-101.

***** TABLE NUMBER 2 *****

Table with 4 columns: NAPL-WATER CAP. PRESSURE, WATER SATURATION, RELATIVE PERM. WATER, RELATIVE PERM. NAPL. Rows 102-124.

Listing of STROUT at 02:52:52 on FEB 5, 1988 for CCID=BBN on UALTIMTS

30000.00000 1.05000 1.00000 0.00000

AIR-NAPL SYSTEM -- PC-KR TABLE NUMBER 2
 NAPL KR AT RESIDUAL WATER SATURATION : 0.50000

AIR-NAPL CAP. PRESSURE	AIR SATURATION	RELATIVE PERM. NAPL	RELATIVE PERM. AIR
5000.00000	1.00000	0.00000	0.00000
0.00000	0.00000	0.00000	0.00000

2 PERMEABILITY SETS WILL BE READ

SET NUMBER	KX	KZ
1	0.10000E-12	0.10000E-12
2	0.10000E-15	0.10000E-15

2 POROSITY SETS WILL BE READ

SET NUMBER	REF. POROSITY	COMPRESSIBILITY	REF. PRESSURE
1	0.20000	0.10000E-05	0.10000E+05
2	0.50000E-01	0.10000E-05	0.10000E+05

GRID BLOCK SPACINGS IN THE X-DIRECTION

5.0000	10.000	50.000	50.000	50.000	50.000	50.000	50.000	50.000	50.000	50.000
5.0000	10.000	50.000	50.000	50.000	50.000	50.000	50.000	50.000	50.000	50.000

GRID BLOCK SPACINGS IN THE Z-DIRECTION

5.0000	25.000	25.000	25.000	25.000	12.500	5.0000	5.0000	5.0000	5.0000
5.0000	25.000	25.000	25.000	25.000	12.500	5.0000	5.0000	5.0000	5.0000

THERE ARE 2 PROPERTY COMBINATION SETS

SET NUMBER	PC-KR TABLE	K CLASS	POROSITY CLASS
1	1	1	1
2	2	2	2

GRID BLOCK NUMBERS

X-DIRECTION ---->

LAYER 1 -1 1 21 51 81 121 151 181 211 241 271 301 331 361 391 421 451 481 511 541 571 601 631 661 691 721 751 781 811 841 871 901 931 961 991 1021 1051 1081 1111 1141 1171 1201 1231 1261 1291 1321 1351 1381 1411 1441

LAYER 2 -1 2 32 62 92 122 152 182 212 242 272 302 332 362 392 422 452 482 512 542 572 602 632 662 692 722 752 782 812 842 872 902 932 962 992 1022 1052 1082 1112 1142 1172 1202 1232 1262 1292 1322 1352 1382 1412 1442

LAYER 3 -1 3 32 63 93 123 153 183 213 243 273 303 333 363 393 423 453 483 513 543 573 603 633 663 693 723 753 783 813 843 873 903 933 963 993 1023 1053 1083 1113 1143 1173 1203 1233 1263 1293 1323 1353 1383 1413 1443

LAYER 4 -1 4 34 64 94 124 154 184 214 244 274 304 334 364 394 424 454 484 514 544 574 604 634 664 694 724 754 784 814 844 874 904 934 964 994 1024 1054 1084 1114 1144 1174 1204 1234 1264 1294 1324 1354 1384 1414 1444

LAYER 5 -1 5 35 65 95 125 155 185 215 245 275 305 335 365 395 425 455 485 515 545 575 605 635 665 695 725 755 785 815 845 875 905 935 965 995 1025 1055 1085 1115 1145 1175 1205 1235 1265 1295 1325 1355 1385 1415 1445

LAYER 6 -1 6 36 66 96 126 156 186 216 246 276 306 336 366 396 426 456 486 516 546 576 606 636 666 696 726 756 786 816 846 876 906 936 966 996 1026 1056 1086 1116 1146 1176 1206 1236 1266 1296 1326 1356 1386 1416 1446

LAYER 7 -1 7 37 67 97 127 157 187 217 247 277 307 337 367 397 427 457 487 517 547 577 607 637 667 697 727 757 787 817 847 877 907 937 967 997 1027 1057 1087 1117 1147 1177 1207 1237 1267 1297 1327 1357 1387 1417 1447

LAYER 8 -1 8 38 68 98 128 158 188 218 248 278 308 338 368 398 428 458 488 518 548 578 608 638 668 698 728 758 788 818 848 878 908 938 968 998 1028 1058 1088 1118 1148 1178 1208 1238 1268 1298 1328 1358 1388 1418 1448

LAYER 9 -1 9 39 69 99 129 159 189 219 249 279 309 339 369 399 429 459 489 519 549 579 609 639 669 699 729 759 789 819 849 879 909 939 969 999 1029 1059 1089 1119 1149 1179 1209 1239 1269 1299 1329 1359 1389 1419 1449

LAYER 10 -1 10 40 70 100 130 160 190 220 250 280 310 340 370 400 430 460 490 520 550 580 610 640 670 700 730 760 790 820 850 880 910 940 970 1000 1030 1060 1090 1120 1150 1180 1210 1240 1270 1300 1330 1360 1390 1420 1450

LAYER 11 -1 11 41 71 101 131 161 191 221 251 281 311 341 371 401 431 461 491 521 551 581 611 641 671 701 731 761 791 821 851 881 911 941 971 1001 1031 1061 1091 1121 1151 1181 1211 1241 1271 1301 1331 1361 1391 1421 1451

LAYER 12 -1 12 42 72 102 132 162 192 222 252 282 312 342 372 402 432 462 492 522 552 582 612 642 672 702 732 762 792 822 852 882 912 942 972 1002 1032 1062 1092 1122 1152 1182 1212 1242 1272 1302 1332 1362 1392 1422 1452

LAYER 13 -1 13 43 73 103 133 163 193 223 253 283 313 343 373 403 433 463 493 523 553 583 613 643 673 703 733 763 793 823 853 883 913 943 973 1003 1033 1063 1093 1123 1153 1183 1213 1243 1273 1303 1333 1363 1393 1423 1453

LAYER 14 -1 14 44 74 104 134 164 194 224 254 284 314 344 374 404 434 464 494 524 554 584 614 644 674 704 734 764 794 824 854 884 914 944 974 1004 1034 1064 1094 1124 1154 1184 1214 1244 1274 1304 1334 1364 1394 1424 1454

LAYER 15 -1 15 45 75 105 135 165 195 225 255 285 315 345 375 405 435 465 495 525 555 585 615 645 675 705 735 765 795 825 855 885 915 945 975 1005 1035 1065 1095 1125 1155 1185 1215 1245 1275 1305 1335 1365 1395 1425 1455

LAYER 16 -1 16 46 76 106 136 166 196 226 256 286 316 346 376 406 436 466 496 526 556 586 616 646 676 706 736 766 796 826 856 886 916 946 976 1006 1036 1066 1096 1126 1156 1186 1216 1246 1276 1306 1336 1366 1396 1426 1456

LAYER 17 -1 17 47 77 107 137 167 197 227 257 287 317 347 377 407 437 467 497 527 557 587 617 647 677 707 737 767 797 827 857 887 917 947 977 1007 1037 1067 1097 1127 1157 1187 1217 1247 1277 1307 1337 1367 1397 1427 1457

LAYER 18 -1 18 48 78 108 138 168 198 228 258 288 318 348 378 408 438 468 498 528 558 588 618 648 678 708 738 768 798 828 858 888 918 948 978 1008 1038 1068 1098 1128 1158 1188 1218 1248 1278 1308 1338 1368 1398 1428 1458

LAYER 19 -1 19 49 79 109 139 169 199 229 259 289 319 349 379 409 439 469 499 529 559 589 619 649 679 709 739 769 799 829 859 889 919 949 979 1009 1039 1069 1099 1129 1159 1189 1219 1249 1279 1309 1339 1369 1399 1429 1459

Listing of ST2DUT at 02:52:52 on FEB 5, 1985 for CCID-BERN on UALTAMTS Page 3

Table with columns for layer numbers (20, 21, 22, 23, 24, 25, 26, 27, 28) and various numerical values representing data points for each layer.

PROPERTY CLASS NUMBERS

Large table with columns for X-DIRECTION (1-25) and I INDEX (1-25), containing numerical data for layers 1 through 28.

Listing of ST20UT at 02:52:52 on FEB 5, 1988 for CCG=BBBR on MALTANTS

Page 4

Table with columns 373-390 and rows showing data for LAYER 28 and LAYER 30.

***** CALCULATED MAXIMUM BANDWIDTH = 123 *****

INITIAL CONDITION DATA

INITIAL NAPL PRESSURES

Main data table with columns 390-415 and rows 390-415, containing numerical values for various layers and conditions.

Listing of STROUT at 02:52:52 on FEB 5, 1988 for CCI0BERR on UALTAITS

Table with columns for layer numbers (e.g., LAYER 18, LAYER 17, LAYER 16, LAYER 15, LAYER 14, LAYER 13, LAYER 12, LAYER 11, LAYER 10, LAYER 9, LAYER 8, LAYER 7, LAYER 6, LAYER 5, LAYER 4, LAYER 3) and corresponding numerical values for each layer.

INITIAL WATER SATURATIONS

Table showing initial water saturations for layers 1 through 3, with columns for layer number and numerical saturation values.

Listing of ST20UV at 02:52:52 on FEB 5, 1988 for CCI=BNR on UALTANTS

745	1.0000	1.0000	1.0000	1.0000	1.0000	1.0000	1.0000	1.0000	1.0000	1.0000	1.0000
746	LAYER 21										
747	1.0000	1.0000	1.0000	1.0000	1.0000	1.0000	1.0000	1.0000	1.0000	1.0000	1.0000
748	1.0000	1.0000	1.0000	1.0000	1.0000	1.0000	1.0000	1.0000	1.0000	1.0000	1.0000
749	1.0000	1.0000	1.0000	1.0000	1.0000	1.0000	1.0000	1.0000	1.0000	1.0000	1.0000
750	1.0000	1.0000	1.0000	1.0000	1.0000	1.0000	1.0000	1.0000	1.0000	1.0000	1.0000
751	1.0000	1.0000	1.0000	1.0000	1.0000	1.0000	1.0000	1.0000	1.0000	1.0000	1.0000
752	1.0000	1.0000	1.0000	1.0000	1.0000	1.0000	1.0000	1.0000	1.0000	1.0000	1.0000
753	LAYER 22										
754	1.0000	1.0000	1.0000	1.0000	1.0000	1.0000	1.0000	1.0000	1.0000	1.0000	1.0000
755	1.0000	1.0000	1.0000	1.0000	1.0000	1.0000	1.0000	1.0000	1.0000	1.0000	1.0000
756	1.0000	1.0000	1.0000	1.0000	1.0000	1.0000	1.0000	1.0000	1.0000	1.0000	1.0000
757	1.0000	1.0000	1.0000	1.0000	1.0000	1.0000	1.0000	1.0000	1.0000	1.0000	1.0000
758	1.0000	1.0000	1.0000	1.0000	1.0000	1.0000	1.0000	1.0000	1.0000	1.0000	1.0000
759	1.0000	1.0000	1.0000	1.0000	1.0000	1.0000	1.0000	1.0000	1.0000	1.0000	1.0000
760	LAYER 23										
761	1.0000	1.0000	1.0000	1.0000	1.0000	1.0000	1.0000	1.0000	1.0000	1.0000	1.0000
762	1.0000	1.0000	1.0000	1.0000	1.0000	1.0000	1.0000	1.0000	1.0000	1.0000	1.0000
763	1.0000	1.0000	1.0000	1.0000	1.0000	1.0000	1.0000	1.0000	1.0000	1.0000	1.0000
764	1.0000	1.0000	1.0000	1.0000	1.0000	1.0000	1.0000	1.0000	1.0000	1.0000	1.0000
765	1.0000	1.0000	1.0000	1.0000	1.0000	1.0000	1.0000	1.0000	1.0000	1.0000	1.0000
766	1.0000	1.0000	1.0000	1.0000	1.0000	1.0000	1.0000	1.0000	1.0000	1.0000	1.0000
767	LAYER 24										
768	1.0000	1.0000	1.0000	1.0000	1.0000	1.0000	1.0000	1.0000	1.0000	1.0000	1.0000
769	1.0000	1.0000	1.0000	1.0000	1.0000	1.0000	1.0000	1.0000	1.0000	1.0000	1.0000
770	1.0000	1.0000	1.0000	1.0000	1.0000	1.0000	1.0000	1.0000	1.0000	1.0000	1.0000
771	1.0000	1.0000	1.0000	1.0000	1.0000	1.0000	1.0000	1.0000	1.0000	1.0000	1.0000
772	1.0000	1.0000	1.0000	1.0000	1.0000	1.0000	1.0000	1.0000	1.0000	1.0000	1.0000
773	1.0000	1.0000	1.0000	1.0000	1.0000	1.0000	1.0000	1.0000	1.0000	1.0000	1.0000
774	LAYER 25										
775	1.0000	1.0000	1.0000	1.0000	1.0000	1.0000	1.0000	1.0000	1.0000	1.0000	1.0000
776	1.0000	1.0000	1.0000	1.0000	1.0000	1.0000	1.0000	1.0000	1.0000	1.0000	1.0000
777	1.0000	1.0000	1.0000	1.0000	1.0000	1.0000	1.0000	1.0000	1.0000	1.0000	1.0000
778	1.0000	1.0000	1.0000	1.0000	1.0000	1.0000	1.0000	1.0000	1.0000	1.0000	1.0000
779	1.0000	1.0000	1.0000	1.0000	1.0000	1.0000	1.0000	1.0000	1.0000	1.0000	1.0000
780	1.0000	1.0000	1.0000	1.0000	1.0000	1.0000	1.0000	1.0000	1.0000	1.0000	1.0000
781	LAYER 26										
782	1.0000	1.0000	1.0000	1.0000	1.0000	1.0000	1.0000	1.0000	1.0000	1.0000	1.0000
783	1.0000	1.0000	1.0000	1.0000	1.0000	1.0000	1.0000	1.0000	1.0000	1.0000	1.0000
784	1.0000	1.0000	1.0000	1.0000	1.0000	1.0000	1.0000	1.0000	1.0000	1.0000	1.0000
785	1.0000	1.0000	1.0000	1.0000	1.0000	1.0000	1.0000	1.0000	1.0000	1.0000	1.0000
786	1.0000	1.0000	1.0000	1.0000	1.0000	1.0000	1.0000	1.0000	1.0000	1.0000	1.0000
787	1.0000	1.0000	1.0000	1.0000	1.0000	1.0000	1.0000	1.0000	1.0000	1.0000	1.0000
788	LAYER 27										
789	1.0000	1.0000	1.0000	1.0000	1.0000	1.0000	1.0000	1.0000	1.0000	1.0000	1.0000
790	1.0000	1.0000	1.0000	1.0000	1.0000	1.0000	1.0000	1.0000	1.0000	1.0000	1.0000
791	1.0000	1.0000	1.0000	1.0000	1.0000	1.0000	1.0000	1.0000	1.0000	1.0000	1.0000
792	1.0000	1.0000	1.0000	1.0000	1.0000	1.0000	1.0000	1.0000	1.0000	1.0000	1.0000
793	1.0000	1.0000	1.0000	1.0000	1.0000	1.0000	1.0000	1.0000	1.0000	1.0000	1.0000
794	1.0000	1.0000	1.0000	1.0000	1.0000	1.0000	1.0000	1.0000	1.0000	1.0000	1.0000
795	LAYER 28										
796	1.0000	1.0000	1.0000	1.0000	1.0000	1.0000	1.0000	1.0000	1.0000	1.0000	1.0000
797	1.0000	1.0000	1.0000	1.0000	1.0000	1.0000	1.0000	1.0000	1.0000	1.0000	1.0000
798	1.0000	1.0000	1.0000	1.0000	1.0000	1.0000	1.0000	1.0000	1.0000	1.0000	1.0000
799	1.0000	1.0000	1.0000	1.0000	1.0000	1.0000	1.0000	1.0000	1.0000	1.0000	1.0000
800	1.0000	1.0000	1.0000	1.0000	1.0000	1.0000	1.0000	1.0000	1.0000	1.0000	1.0000
801	1.0000	1.0000	1.0000	1.0000	1.0000	1.0000	1.0000	1.0000	1.0000	1.0000	1.0000
802	LAYER 29										
803	1.0000	1.0000	1.0000	1.0000	1.0000	1.0000	1.0000	1.0000	1.0000	1.0000	1.0000
804	1.0000	1.0000	1.0000	1.0000	1.0000	1.0000	1.0000	1.0000	1.0000	1.0000	1.0000
805	1.0000	1.0000	1.0000	1.0000	1.0000	1.0000	1.0000	1.0000	1.0000	1.0000	1.0000
806	1.0000	1.0000	1.0000	1.0000	1.0000	1.0000	1.0000	1.0000	1.0000	1.0000	1.0000
807	1.0000	1.0000	1.0000	1.0000	1.0000	1.0000	1.0000	1.0000	1.0000	1.0000	1.0000
808	1.0000	1.0000	1.0000	1.0000	1.0000	1.0000	1.0000	1.0000	1.0000	1.0000	1.0000
809	LAYER 30										
810	1.0000	1.0000	1.0000	1.0000	1.0000	1.0000	1.0000	1.0000	1.0000	1.0000	1.0000
811	1.0000	1.0000	1.0000	1.0000	1.0000	1.0000	1.0000	1.0000	1.0000	1.0000	1.0000
812	1.0000	1.0000	1.0000	1.0000	1.0000	1.0000	1.0000	1.0000	1.0000	1.0000	1.0000
813	1.0000	1.0000	1.0000	1.0000	1.0000	1.0000	1.0000	1.0000	1.0000	1.0000	1.0000
814	1.0000	1.0000	1.0000	1.0000	1.0000	1.0000	1.0000	1.0000	1.0000	1.0000	1.0000
815	1.0000	1.0000	1.0000	1.0000	1.0000	1.0000	1.0000	1.0000	1.0000	1.0000	1.0000

RECURRENT DATA SET

INITIAL TIME STEP SIZE = 0.55400E+05
 MINIMUM TIME STEP SIZE = 3000.0
 MAXIMUM WATER SATURATION CHANGE = 0.10000
 TIME STEP MULTIPLIER = 1.2500
 TIME TO READ NEW RECURRENT DATA = 0.10000E+17
 NUMBER OF SOURCE/SINK BLOCKS = 0
 CODE FOR CHANGING FLUX RATES = 0

TIME STEP NUMBER = 1 TIME VALUE = 0.55400E+05

CONSTANT PRES	WATER BALANCE	NAPL BALANCE
SOURCE/SINKS	2.7824	0.00000E+00
STORAGE	0.00000E+00	0.00000E+00
PER CENT ERROR	-2.7824	0.00000E+00

STEP NUMBER 1 COMPLETED SIMULATION TIME IN SECONDS 0.554E+05
 IN MINUTES 0.924E+03
 IN HOURS 2.0
 IN DAYS 10.00
 IN YEARS 0.274E-01

TIME STEP NUMBER = 2 TIME VALUE = 0.10440E+07

CONSTANT PRES	WATER BALANCE	NAPL BALANCE
SOURCE/SINKS	2.7872	0.00000E+00
STORAGE	0.00000E+00	0.00000E+00
PER CENT ERROR	-2.7872	0.00000E+00

STEP NUMBER 2 COMPLETED SIMULATION TIME IN SECONDS 0.1044E+07
 IN MINUTES 0.174E+05
 IN HOURS 540
 IN DAYS 22.5
 IN YEARS 0.618E-01

TIME STEP NUMBER = 3 TIME VALUE = 0.32040E+07

CONSTANT PRES	WATER BALANCE	NAPL BALANCE
SOURCE/SINKS	2.7275	0.00000E+00
STORAGE	0.00000E+00	0.00000E+00

Appendix 3

Sample Computer Output, Case Two.

Listing of STROUT at 02:12:23 on FEB 5, 1988 for CCID=SENR on UALTANTS

S W A M F L O W - 2 D

SIMULTANEOUS WATER, AIR, AND NAPL FLOW IN TWO DIMENSIONS

WRITTEN BY:

CHARLES R. FAUST
JAMES D. RUMBAUGH

GEOTRANS, INC.
260 EXCHANGE PLACE
SUITE A
MERIDON, VA

LENS 10:1 RADIENT = 0.02 EPSILON = 1000 ----STEADY STATE----
DATE 02 FEB 1988 RUN NO 7_1

NUMBER OF BLOCKS IN THE X-DIRECTION (COLUMNS) = 50
NUMBER OF BLOCKS IN THE Z-DIRECTION (LAYERS) = 20
MAXIMUM OF NEWTON-RAPHSON ITERATIONS = 5
MAXIMUM BANDWIDTH = 50
MAXIMUM NUMBER OF TIME STEPS = 1740
NUMBER OF ACTIVE GRID BLOCKS = 50
NUMBER OF TIME STEPS BETWEEN PRINTOUTS = 1
PRINT NAPL AND WATER POTENTIALS? (Y/N) = 0
PRINT DETAILED KR TABLES? (Y/N) = 1
WRITE A PLOT FILE? (Y/N) = 0
NUMBER OF OBSERVATION BLOCKS = 1
WRITE A RESTART FILE? (Y/N) = 1

GRID BLOCK THICKNESS (DY) = 1.0000
MASS BALANCE TOLERANCE FOR NEWTON-RAPHSON IT. = 0.10000E-01
INITIAL TIME VALUE = 0.00000E+00
WATER DENSITY = 1000.0
NAPL DENSITY = 850.00
WATER VISCOSITY = 0.10000E-02
NAPL VISCOSITY = 0.20000E-02
GRAVITATIONAL CONSTANT IN THE Z-DIRECTION = -9.8100
GRAVITATIONAL CONSTANT IN THE X-DIRECTION = 0.00000E+00

2 PC-KR TABLES WILL BE READ

***** TABLE NUMBER 1 *****

NAPL-WATER CAP. PRESSURE	WATER SATURATION	RELATIVE PERM. WATER	RELATIVE PERM. NAPL
240000.00000	0.00000	0.00000	1.00000
240000.00000	0.00000	0.00000	1.00000
240000.00000	0.00000	0.00000	1.00000
240000.00000	0.10000	0.00000	1.00000
240000.00000	0.20000	0.00000	1.00000
240000.00000	0.30000	0.00000	1.00000
240000.00000	0.40000	0.00000	1.00000
240000.00000	0.50000	0.00000	1.00000
240000.00000	0.60000	0.00000	1.00000
240000.00000	0.70000	0.00000	1.00000
240000.00000	0.80000	0.00000	1.00000
240000.00000	0.90000	0.00000	1.00000
240000.00000	1.00000	0.00000	1.00000

AIR-NAPL SYSTEM -- PC-KR TABLE NUMBER 1
NAPL KR AT RESIDUAL WATER SATURATION : 0.50000

AIR-NAPL CAP. PRESSURE	AIR SATURATION	RELATIVE PERM. NAPL	RELATIVE PERM. AIR
0.00000	1.00000	0.00000	0.00000
0.00000	0.00000	0.00000	0.00000

***** TABLE NUMBER 2 *****

NAPL-WATER CAP. PRESSURE	WATER SATURATION	RELATIVE PERM. WATER	RELATIVE PERM. NAPL
480000.00000	0.00000	0.00000	1.00000
480000.00000	0.00000	0.00000	1.00000
480000.00000	0.05000	0.00000	1.00000
480000.00000	0.10000	0.00000	1.00000
480000.00000	0.15000	0.00000	1.00000
480000.00000	0.20000	0.00000	1.00000
480000.00000	0.25000	0.00000	1.00000
480000.00000	0.30000	0.00000	1.00000
480000.00000	0.35000	0.00000	1.00000
480000.00000	0.40000	0.00000	1.00000
480000.00000	0.45000	0.00000	1.00000
480000.00000	0.50000	0.00000	1.00000
480000.00000	0.55000	0.01200	0.21000
480000.00000	0.60000	0.02500	0.12000
480000.00000	0.65000	0.03700	0.06000
480000.00000	0.70000	0.04700	0.03500
480000.00000	0.75000	0.05200	0.02500
480000.00000	0.80000	0.05000	0.01800
480000.00000	0.85000	0.04000	0.01000
480000.00000	0.90000	0.02500	0.00500
480000.00000	0.95000	0.01000	0.00200
480000.00000	1.00000	0.00000	0.00000

125	30000.00000	1.05000	1.00000	0.00000
126	AIR-NAPL SYSTEM -- PC-KR TABLE NUMBER 2			
127	NAPL KR AT RESIDUAL WATER SATURATION : 0.88000			
128				
129	AIR-NAPL CAP.	AIR	RELATIVE PERM.	RELATIVE PERM.
130	PRESSURE	SATURATION	NAPL	AIR
131	-5500.00000	1.00000	0.00000	0.00000
132	0.00000	0.00000	0.00000	0.00000

2 PERMEABILITY SETS WILL BE READ

142	SET NUMBER	KK	KZ
143	1	0.10000E-12	0.10000E-12
144	2	0.10000E-15	0.10000E-15

2 POROSITY SETS WILL BE READ

151	SET NUMBER	REP. POROSITY	COMPRESSIBILITY	REP. PRESSURE
152	1	0.20000	0.10000E-08	0.10000E+08
153	2	0.50000E-01	0.10000E-08	0.10000E+08

GRID BLOCK SPACINGS IN THE X-DIRECTION

158	5.0000	10.0000	50.0000	50.0000	50.0000	50.0000	50.0000	50.0000	50.0000	50.0000
159	25.0000	20.0000	10.0000	10.0000	10.0000	10.0000	10.0000	10.0000	10.0000	10.0000
160	5.0000	5.0000	5.0000	5.0000	5.0000	5.0000	5.0000	5.0000	5.0000	5.0000
161	5.0000	15.0000	15.0000	15.0000	15.0000	15.0000	15.0000	15.0000	15.0000	15.0000
162	5.0000	5.0000	5.0000	5.0000	5.0000	5.0000	5.0000	5.0000	5.0000	5.0000
163	5.0000	5.0000	5.0000	5.0000	5.0000	5.0000	5.0000	5.0000	5.0000	5.0000
164	5.0000	5.0000	5.0000	5.0000	5.0000	5.0000	5.0000	5.0000	5.0000	5.0000
165	5.0000	5.0000	5.0000	5.0000	5.0000	5.0000	5.0000	5.0000	5.0000	5.0000
166	5.0000	5.0000	5.0000	5.0000	5.0000	5.0000	5.0000	5.0000	5.0000	5.0000

GRID BLOCK SPACINGS IN THE Z-DIRECTION

172	5.0000	25.0000	25.0000	25.0000	25.0000	12.5000	5.0000	5.0000	5.0000	5.0000
173	2.5000	2.5000	2.5000	2.5000	2.5000	2.5000	2.5000	2.5000	2.5000	2.5000
174	5.0000	5.0000	5.0000	5.0000	5.0000	5.0000	5.0000	5.0000	5.0000	5.0000

THERE ARE 2 PROPERTY COMBINATION SETS

180	SET NUMBER	PC-KR TABLE	K CLASS	POROSITY CLASS
181	1	1	1	1
182	2	2	2	2

GRID BLOCK NUMBERS

X-DIRECTION ---->

187	LAYER 1	-1	1	31	51	51	121	151	151	211	241	271	301	331	361	391	421	451	481	511	541	571	601	631	661	691
188		721	751	781	811	841	871	901	931	961	991	1021	1051	1081	1111	1141	1171	1201	1231	1261	1291	1321	1351	1381	1411	1441
189	LAYER 2	-1	2	32	62	92	122	152	182	212	242	272	302	332	362	392	422	452	482	512	542	572	602	632	662	692
190		722	752	782	812	842	872	902	932	962	992	1022	1052	1082	1112	1142	1172	1202	1232	1262	1292	1322	1352	1382	1412	1442
191	LAYER 3	-1	3	33	63	93	123	153	183	213	243	273	303	333	363	393	423	453	483	513	543	573	603	633	663	693
192		723	753	783	813	843	873	903	933	963	993	1023	1053	1083	1113	1143	1173	1203	1233	1263	1293	1323	1353	1383	1413	1443
193	LAYER 4	-1	4	34	64	94	124	154	184	214	244	274	304	334	364	394	424	454	484	514	544	574	604	634	664	694
194		724	754	784	814	844	874	904	934	964	994	1024	1054	1084	1114	1144	1174	1204	1234	1264	1294	1324	1354	1384	1414	1444
195	LAYER 5	-1	5	35	65	95	125	155	185	215	245	275	305	335	365	395	425	455	485	515	545	575	605	635	665	695
196		725	755	785	815	845	875	905	935	965	995	1025	1055	1085	1115	1145	1175	1205	1235	1265	1295	1325	1355	1385	1415	1445
197	LAYER 6	-1	6	36	66	96	126	156	186	216	246	276	306	336	366	396	426	456	486	516	546	576	606	636	666	696
198		726	756	786	816	846	876	906	936	966	996	1026	1056	1086	1116	1146	1176	1206	1236	1266	1296	1326	1356	1386	1416	1446
199	LAYER 7	-1	7	37	67	97	127	157	187	217	247	277	307	337	367	397	427	457	487	517	547	577	607	637	667	697
200		727	757	787	817	847	877	907	937	967	997	1027	1057	1087	1117	1147	1177	1207	1237	1267	1297	1327	1357	1387	1417	1447
201	LAYER 8	-1	8	38	68	98	128	158	188	218	248	278	308	338	368	398	428	458	488	518	548	578	608	638	668	698
202		728	758	788	818	848	878	908	938	968	998	1028	1058	1088	1118	1148	1178	1208	1238	1268	1298	1328	1358	1388	1418	1448
203	LAYER 9	-1	9	39	69	99	129	159	189	219	249	279	309	339	369	399	429	459	489	519	549	579	609	639	669	699
204		729	759	789	819	849	879	909	939	969	999	1029	1059	1089	1119	1149	1179	1209	1239	1269	1299	1329	1359	1389	1419	1449
205	LAYER 10	-1	10	40	70	100	130	160	190	220	250	280	310	340	370	400	430	460	490	520	550	580	610	640	670	700
206		730	760	790	820	850	880	910	940	970	1000	1030	1060	1090	1120	1150	1180	1210	1240	1270	1300	1330	1360	1390	1420	1450
207	LAYER 11	-1	11	41	71	101	131	161	191	221	251	281	311	341	371	401	431	461	491	521	551	581	611	641	671	701
208		731	761	791	821	851	881	911	941	971	1001	1031	1061	1091	1121	1151	1181	1211	1241	1271	1301	1331	1361	1391	1421	1451
209	LAYER 12	-1	12	42	72	102	132	162	192	222	252	282	312	342	372	402	432	462	492	522	552	582	612	642	672	702
210		732	762	792	822	852	882	912	942	972	1002	1032	1062	1092	1122	1152	1182	1212	1242	1272	1302	1332	1362	1392	1422	1452
211	LAYER 13	-1	13	43	73	103	133	163	193	223	253	283	313	343	373	403	433	463	493	523	553	583	613	643	673	703
212		733	763	793	823	853	883	913	943	973	1003	1033	1063	1093	1123	1153	1183	1213	1243	1273	1303	1333	1363	1393	1423	1453
213	LAYER 14	-1	14	44	74	104	134	164	194	224	254	284	314	344	374	404	434	464	494	524	554	584	614	644	674	704
214		734	764	794	824	854	884	914	944	974	1004	1034	1064	1094	1124	1154	1184	1214	1244	1274	1304	1334	1364	1394	1424	1454
215	LAYER 15	-1	15	45	75	105	135	165	195	225	255	285	315	345	375	405	435	465	495	525	555	585	615	645	675	705
216		735	765	795	825	855	885	915	945	975	1005	1035	1065	1095	1125	1155	1185	1215	1245	1275	1305	1335	1365	1395	1425	1455
217	LAYER 16	-1	16	46	76	106	136	166	196	226	256	286	316	346	376	406	436	466	496	526	556	586	616	646	676	706
218		736	766	796	826	856	886	916	946	976	1006	1036	1066	1096	1126	1156	1186	1216	1246	1276	1306	1336	1366	1396	1426	1456
219	LAYER 17	-1	17	47	77	107	137	167	197	227	257	287	317	347	377	407	437	467	497	527	557	587	617	647	677	707
220		737	767	797	827	857	887	917	947	977	1007	1037	1067	1097	1127	1157	1187	1217	1247	1277	1307	1337	1367	1397	1427	1457
221	LAYER 18	-1	18	48	78	108	138	168	198	228	258	288	318	348	378	408	438	468	498	528	558	588	618	648	678	708
222		738	768	798	828	858	888	918	948	978	1008	1038	1068	1098	1128	1158	1188	1218	1248	1278	1308	1338	1368	1398	1	

Listing of STROUT at 02:22:28 on FEB 8, 1988 for CCIDBERR on UALMANTS

Page 8

487	LAYER 16	0.73752E+07	0.73757E+07	0.73822E+07	0.73824E+07	0.74022E+07	0.74120E+07	0.74218E+07	0.74316E+07	0.74414E+07	0.74512E+07	0.74610E+07
488		0.74512E+07	0.74517E+07	0.74582E+07	0.74584E+07	0.74782E+07	0.74880E+07	0.74978E+07	0.75076E+07	0.75174E+07	0.75272E+07	0.75370E+07
489		0.75370E+07	0.75375E+07	0.75440E+07	0.75442E+07	0.75640E+07	0.75738E+07	0.75836E+07	0.75934E+07	0.76032E+07	0.76130E+07	0.76228E+07
490		0.76228E+07	0.76233E+07	0.76300E+07	0.76302E+07	0.76500E+07	0.76598E+07	0.76696E+07	0.76794E+07	0.76892E+07	0.76990E+07	0.77088E+07
491		0.77088E+07	0.77093E+07	0.77160E+07	0.77162E+07	0.77360E+07	0.77458E+07	0.77556E+07	0.77654E+07	0.77752E+07	0.77850E+07	0.77948E+07
492		0.77948E+07	0.77953E+07	0.78020E+07	0.78022E+07	0.78220E+07	0.78318E+07	0.78416E+07	0.78514E+07	0.78612E+07	0.78710E+07	0.78808E+07
493		0.78808E+07	0.78813E+07	0.78880E+07	0.78882E+07	0.79080E+07	0.79178E+07	0.79276E+07	0.79374E+07	0.79472E+07	0.79570E+07	0.79668E+07
494		0.79668E+07	0.79673E+07	0.79740E+07	0.79742E+07	0.79940E+07	0.80038E+07	0.80136E+07	0.80234E+07	0.80332E+07	0.80430E+07	0.80528E+07
495		0.80528E+07	0.80533E+07	0.80600E+07	0.80602E+07	0.80800E+07	0.80898E+07	0.80996E+07	0.81094E+07	0.81192E+07	0.81290E+07	0.81388E+07
496		0.81388E+07	0.81393E+07	0.81460E+07	0.81462E+07	0.81660E+07	0.81758E+07	0.81856E+07	0.81954E+07	0.82052E+07	0.82150E+07	0.82248E+07
497		0.82248E+07	0.82253E+07	0.82320E+07	0.82322E+07	0.82520E+07	0.82618E+07	0.82716E+07	0.82814E+07	0.82912E+07	0.83010E+07	0.83108E+07
498		0.83108E+07	0.83113E+07	0.83180E+07	0.83182E+07	0.83380E+07	0.83478E+07	0.83576E+07	0.83674E+07	0.83772E+07	0.83870E+07	0.83968E+07
499		0.83968E+07	0.83973E+07	0.84040E+07	0.84042E+07	0.84240E+07	0.84338E+07	0.84436E+07	0.84534E+07	0.84632E+07	0.84730E+07	0.84828E+07
500		0.84828E+07	0.84833E+07	0.84900E+07	0.84902E+07	0.85100E+07	0.85198E+07	0.85296E+07	0.85394E+07	0.85492E+07	0.85590E+07	0.85688E+07
501		0.85688E+07	0.85693E+07	0.85760E+07	0.85762E+07	0.85960E+07	0.86058E+07	0.86156E+07	0.86254E+07	0.86352E+07	0.86450E+07	0.86548E+07
502		0.86548E+07	0.86553E+07	0.86620E+07	0.86622E+07	0.86820E+07	0.86918E+07	0.87016E+07	0.87114E+07	0.87212E+07	0.87310E+07	0.87408E+07
503		0.87408E+07	0.87413E+07	0.87480E+07	0.87482E+07	0.87680E+07	0.87778E+07	0.87876E+07	0.87974E+07	0.88072E+07	0.88170E+07	0.88268E+07
504		0.88268E+07	0.88273E+07	0.88340E+07	0.88342E+07	0.88540E+07	0.88638E+07	0.88736E+07	0.88834E+07	0.88932E+07	0.89030E+07	0.89128E+07
505		0.89128E+07	0.89133E+07	0.89200E+07	0.89202E+07	0.89400E+07	0.89498E+07	0.89596E+07	0.89694E+07	0.89792E+07	0.89890E+07	0.89988E+07
506		0.89988E+07	0.89993E+07	0.90060E+07	0.90062E+07	0.90260E+07	0.90358E+07	0.90456E+07	0.90554E+07	0.90652E+07	0.90750E+07	0.90848E+07
507		0.90848E+07	0.90853E+07	0.90920E+07	0.90922E+07	0.91120E+07	0.91218E+07	0.91316E+07	0.91414E+07	0.91512E+07	0.91610E+07	0.91708E+07
508		0.91708E+07	0.91713E+07	0.91780E+07	0.91782E+07	0.91980E+07	0.92078E+07	0.92176E+07	0.92274E+07	0.92372E+07	0.92470E+07	0.92568E+07
509		0.92568E+07	0.92573E+07	0.92640E+07	0.92642E+07	0.92840E+07	0.92938E+07	0.93036E+07	0.93134E+07	0.93232E+07	0.93330E+07	0.93428E+07
510		0.93428E+07	0.93433E+07	0.93500E+07	0.93502E+07	0.93700E+07	0.93798E+07	0.93896E+07	0.93994E+07	0.94092E+07	0.94190E+07	0.94288E+07
511		0.94288E+07	0.94293E+07	0.94360E+07	0.94362E+07	0.94560E+07	0.94658E+07	0.94756E+07	0.94854E+07	0.94952E+07	0.95050E+07	0.95148E+07
512		0.95148E+07	0.95153E+07	0.95220E+07	0.95222E+07	0.95420E+07	0.95518E+07	0.95616E+07	0.95714E+07	0.95812E+07	0.95910E+07	0.96008E+07
513		0.96008E+07	0.96013E+07	0.96080E+07	0.96082E+07	0.96280E+07	0.96378E+07	0.96476E+07	0.96574E+07	0.96672E+07	0.96770E+07	0.96868E+07
514		0.96868E+07	0.96873E+07	0.96940E+07	0.96942E+07	0.97140E+07	0.97238E+07	0.97336E+07	0.97434E+07	0.97532E+07	0.97630E+07	0.97728E+07
515		0.97728E+07	0.97733E+07	0.97800E+07	0.97802E+07	0.98000E+07	0.98098E+07	0.98196E+07	0.98294E+07	0.98392E+07	0.98490E+07	0.98588E+07
516		0.98588E+07	0.98593E+07	0.98660E+07	0.98662E+07	0.98860E+07	0.98958E+07	0.99056E+07	0.99154E+07	0.99252E+07	0.99350E+07	0.99448E+07
517		0.99448E+07	0.99453E+07	0.99520E+07	0.99522E+07	0.99720E+07	0.99818E+07	0.99916E+07	1.00014E+07	1.00112E+07	1.00210E+07	1.00308E+07
518		1.00308E+07	1.00313E+07	1.00380E+07	1.00382E+07	1.00580E+07	1.00678E+07	1.00776E+07	1.00874E+07	1.00972E+07	1.01070E+07	1.01168E+07
519		1.01168E+07	1.01173E+07	1.01240E+07	1.01242E+07	1.01440E+07	1.01538E+07	1.01636E+07	1.01734E+07	1.01832E+07	1.01930E+07	1.02028E+07
520		1.02028E+07	1.02033E+07	1.02100E+07	1.02102E+07	1.02300E+07	1.02398E+07	1.02496E+07	1.02594E+07	1.02692E+07	1.02790E+07	1.02888E+07
521		1.02888E+07	1.02893E+07	1.02960E+07	1.02962E+07	1.03160E+07	1.03258E+07	1.03356E+07	1.03454E+07	1.03552E+07	1.03650E+07	1.03748E+07
522		1.03748E+07	1.03753E+07	1.03820E+07	1.03822E+07	1.04020E+07	1.04118E+07	1.04216E+07	1.04314E+07	1.04412E+07	1.04510E+07	1.04608E+07
523		1.04608E+07	1.04613E+07	1.04680E+07	1.04682E+07	1.04880E+07	1.04978E+07	1.05076E+07	1.05174E+07	1.05272E+07	1.05370E+07	1.05468E+07
524		1.05468E+07	1.05473E+07	1.05540E+07	1.05542E+07	1.05740E+07	1.05838E+07	1.05936E+07	1.06034E+07	1.06132E+07	1.06230E+07	1.06328E+07
525		1.06328E+07	1.06333E+07	1.06400E+07	1.06402E+07	1.06600E+07	1.06698E+07	1.06796E+07	1.06894E+07	1.06992E+07	1.07090E+07	1.07188E+07
526		1.07188E+07	1.07193E+07	1.07260E+07	1.07262E+07	1.07460E+07	1.07558E+07	1.07656E+07	1.07754E+07	1.07852E+07	1.07950E+07	1.08048E+07
527		1.08048E+07	1.08053E+07	1.08120E+07	1.08122E+07	1.08320E+07	1.08418E+07	1.08516E+07	1.08614E+07	1.08712E+07	1.08810E+07	1.08908E+07
528		1.08908E+07	1.08913E+07	1.08980E+07	1.08982E+07	1.09180E+07	1.09278E+07	1.09376E+07	1.09474E+07	1.09572E+07	1.09670E+07	1.09768E+07
529		1.09768E+07	1.09773E+07	1.09840E+07	1.09842E+07	1.10040E+07	1.10138E+07	1.10236E+07	1.10334E+07	1.10432E+07	1.10530E+07	1.10628E+07
530		1.10628E+07	1.10633E+07	1.10700E+07	1.10702E+07	1.10900E+07	1.10998E+07	1.11096E+07	1.11194E+07	1.11292E+07	1.11390E+07	1.11488E+07
531		1.11488E+07	1.11493E+07	1.11560E+07	1.11562E+07	1.11760E+07	1.11858E+07	1.11956E+07	1.12054E+07	1.12152E+07	1.12250E+07	1.12348E+07
532		1.12348E+07	1.12353E+07	1.12420E+07	1.12422E+07	1.12620E+07	1.12718E+07	1.12816E+07	1.12914E+07	1.13012E+07	1.13110E+07	1.13208E+07
533		1.13208E+07	1.13213E+07	1.13280E+07	1.13282E+07	1.13480E+07	1.13578E+07	1.13676E+07	1.13774E+07	1.13872E+07	1.13970E+07	1.14068E+07
534		1.14068E+07	1.14073E+07	1.14140E+07	1.14142E+07	1.14340E+07	1.14438E+07	1.14536E+07	1.14634E+07	1.14732E+07	1.14830E+07	1.14928E+07
535		1.14928E+07	1.14933E+07	1.15000E+07	1.15002E+07	1.15200E+07	1.15298E+07	1.15396E+07	1.15494E+07	1.15592E+07	1.15690E+07	1.15788E+07
536		1.15788E+07	1.15793E+07	1.15860E+07	1.15862E+07	1.16060E+07	1.16158E+07	1.16256E+07	1.16354E+07	1.16452E+07	1.16550E+07	1.16648E+07
537		1.16648E+07	1.16653E+07	1.16720E+07	1.16722E+07	1.16920E+07	1.17018E+07	1.17116E+07	1.17214E+07	1.17312E+07	1.17410E+07	1.17508E+07
538		1.17508E+07	1.17513E+07	1.17580E+07	1.17582E+07	1.17780E+07	1.17878E+07	1.17976E+07	1.18074E+07	1.18172E+07	1.18270E+07	1.18368E+07
539		1.18368E+07	1.18373E+07	1.18440E+07	1.18442E+07	1.18640E+07	1.18738E+07	1.18836E+07	1.18934E+07	1.19032E+07	1.19130E+07	1.19228E+07
540		1.19228E+07	1.19233E+07	1.19300E+07	1.19302E+07	1.19500E+07	1.19598E+07	1.19696E+07	1.19794E+07	1.19892E+07	1.19990E+07	2.00088E+07
541		2.00088E+07	2.00093E+07	2.00160E+07	2.00162E+07	2.00360E+07	2.00458E+07	2.00556E+07	2.00654E+07	2.00752E+07	2.00850E+07	2.00948E+07
542		2.00948E+07	2.00953E+07	2.01020E+07	2.01022E+07	2.01220E+07	2.01318E+07	2.01416E+07	2.01514E+07	2.01612E+07	2.01710E+07	2.01808E+07
543		2.01808E+07	2.01813E+07	2.01880E+07	2.01882E+07	2.02080E+07	2.02178E+07	2.02276E+07	2.02374E+07	2.02472E+07	2.02570E+07	2.02668E+07
544		2.02668E+07	2.02673E+07	2.02740E+07	2.02742E+07	2.02940E+07	2.03038E+07	2.03136E+07	2.03234E+07	2.03332E+07	2.03430E+07	2.03528E+07
545		2.03528E+07	2.03533E+07	2.03600E+07	2.03602E+07	2.03800E+07	2.03898E+07	2.03996E+07	2.04094E+07	2.04192E+07	2.04290E+07	2.04388E+07
546		2.04388E+07	2.04393E+07	2.04460E+07	2.04462E+07	2.04660E+07	2.04758E+07	2.04856E+07	2.04954E+07	2.05052E+07	2.05150E+07	2.05248E+07
547		2.05248E+07	2.05253E+07	2.05320E+07	2.05322E+07	2.05520E+07	2.05618E+07	2.05716E+07	2.05814E+07	2.05912E+07	2.06010E+07	2.06108E+07
548		2.06108E+07	2.06113E+07	2.06180E+07	2.06182E+07	2.06380E+07	2.06478E+07	2.06576E+07	2.06674E+07	2.06772E+07	2.06870E+07	2.06968E+07
549		2.06968E+07	2.06973E+07	2.07040E+07	2.07042E+07	2.07240E+07	2.07338E+07	2.07436E+07	2.07534E+07	2.07632E+07	2.07730E+07	2.07828E+07
550		2.07828E+07	2.07833E									

Listing of STROUT at 02:02:26 on FEB 5, 1988 for CCID=BRN on UALANTS

Page 7

745	1.0000	1.0000	1.0000	1.0000	1.0000	1.0000	1.0000	1.0000	1.0000	1.0000	1.0000
746	LAYER 21										
747	1.0000	1.0000	1.0000	1.0000	1.0000	1.0000	1.0000	1.0000	1.0000	1.0000	1.0000
748	1.0000	1.0000	1.0000	1.0000	1.0000	1.0000	1.0000	1.0000	1.0000	1.0000	1.0000
749	1.0000	1.0000	1.0000	1.0000	1.0000	1.0000	1.0000	1.0000	1.0000	1.0000	1.0000
750	1.0000	1.0000	1.0000	1.0000	1.0000	1.0000	1.0000	1.0000	1.0000	1.0000	1.0000
751	1.0000	1.0000	1.0000	1.0000	1.0000	1.0000	1.0000	1.0000	1.0000	1.0000	1.0000
752	1.0000	1.0000	1.0000	1.0000	1.0000	1.0000	1.0000	1.0000	1.0000	1.0000	1.0000
753	LAYER 22										
754	1.0000	1.0000	1.0000	1.0000	1.0000	1.0000	1.0000	1.0000	1.0000	1.0000	1.0000
755	1.0000	1.0000	1.0000	1.0000	1.0000	1.0000	1.0000	1.0000	1.0000	1.0000	1.0000
756	1.0000	1.0000	1.0000	1.0000	1.0000	1.0000	1.0000	1.0000	1.0000	1.0000	1.0000
757	1.0000	1.0000	1.0000	1.0000	1.0000	1.0000	1.0000	1.0000	1.0000	1.0000	1.0000
758	1.0000	1.0000	1.0000	1.0000	1.0000	1.0000	1.0000	1.0000	1.0000	1.0000	1.0000
759	LAYER 23										
760	1.0000	1.0000	1.0000	1.0000	1.0000	1.0000	1.0000	1.0000	1.0000	1.0000	1.0000
761	1.0000	1.0000	1.0000	1.0000	1.0000	1.0000	1.0000	1.0000	1.0000	1.0000	1.0000
762	1.0000	1.0000	1.0000	1.0000	1.0000	1.0000	1.0000	1.0000	1.0000	1.0000	1.0000
763	1.0000	1.0000	1.0000	1.0000	1.0000	1.0000	1.0000	1.0000	1.0000	1.0000	1.0000
764	1.0000	1.0000	1.0000	1.0000	1.0000	1.0000	1.0000	1.0000	1.0000	1.0000	1.0000
765	1.0000	1.0000	1.0000	1.0000	1.0000	1.0000	1.0000	1.0000	1.0000	1.0000	1.0000
766	1.0000	1.0000	1.0000	1.0000	1.0000	1.0000	1.0000	1.0000	1.0000	1.0000	1.0000
767	LAYER 24										
768	1.0000	1.0000	1.0000	1.0000	1.0000	1.0000	1.0000	1.0000	1.0000	1.0000	1.0000
769	1.0000	1.0000	1.0000	1.0000	1.0000	1.0000	1.0000	1.0000	1.0000	1.0000	1.0000
770	1.0000	1.0000	1.0000	1.0000	1.0000	1.0000	1.0000	1.0000	1.0000	1.0000	1.0000
771	1.0000	1.0000	1.0000	1.0000	1.0000	1.0000	1.0000	1.0000	1.0000	1.0000	1.0000
772	1.0000	1.0000	1.0000	1.0000	1.0000	1.0000	1.0000	1.0000	1.0000	1.0000	1.0000
773	1.0000	1.0000	1.0000	1.0000	1.0000	1.0000	1.0000	1.0000	1.0000	1.0000	1.0000
774	LAYER 25										
775	1.0000	1.0000	1.0000	1.0000	1.0000	1.0000	1.0000	1.0000	1.0000	1.0000	1.0000
776	1.0000	1.0000	1.0000	1.0000	1.0000	1.0000	1.0000	1.0000	1.0000	1.0000	1.0000
777	1.0000	1.0000	1.0000	1.0000	1.0000	1.0000	1.0000	1.0000	1.0000	1.0000	1.0000
778	1.0000	1.0000	1.0000	1.0000	1.0000	1.0000	1.0000	1.0000	1.0000	1.0000	1.0000
779	1.0000	1.0000	1.0000	1.0000	1.0000	1.0000	1.0000	1.0000	1.0000	1.0000	1.0000
780	1.0000	1.0000	1.0000	1.0000	1.0000	1.0000	1.0000	1.0000	1.0000	1.0000	1.0000
781	LAYER 26										
782	1.0000	1.0000	1.0000	1.0000	1.0000	1.0000	1.0000	1.0000	1.0000	1.0000	1.0000
783	1.0000	1.0000	1.0000	1.0000	1.0000	1.0000	1.0000	1.0000	1.0000	1.0000	1.0000
784	1.0000	1.0000	1.0000	1.0000	1.0000	1.0000	1.0000	1.0000	1.0000	1.0000	1.0000
785	1.0000	1.0000	1.0000	1.0000	1.0000	1.0000	1.0000	1.0000	1.0000	1.0000	1.0000
786	1.0000	1.0000	1.0000	1.0000	1.0000	1.0000	1.0000	1.0000	1.0000	1.0000	1.0000
787	1.0000	1.0000	1.0000	1.0000	1.0000	1.0000	1.0000	1.0000	1.0000	1.0000	1.0000
788	LAYER 27										
789	1.0000	1.0000	1.0000	1.0000	1.0000	1.0000	1.0000	1.0000	1.0000	1.0000	1.0000
790	1.0000	1.0000	1.0000	1.0000	1.0000	1.0000	1.0000	1.0000	1.0000	1.0000	1.0000
791	1.0000	1.0000	1.0000	1.0000	1.0000	1.0000	1.0000	1.0000	1.0000	1.0000	1.0000
792	1.0000	1.0000	1.0000	1.0000	1.0000	1.0000	1.0000	1.0000	1.0000	1.0000	1.0000
793	1.0000	1.0000	1.0000	1.0000	1.0000	1.0000	1.0000	1.0000	1.0000	1.0000	1.0000
794	1.0000	1.0000	1.0000	1.0000	1.0000	1.0000	1.0000	1.0000	1.0000	1.0000	1.0000
795	LAYER 28										
796	1.0000	1.0000	1.0000	1.0000	1.0000	1.0000	1.0000	1.0000	1.0000	1.0000	1.0000
797	1.0000	1.0000	1.0000	1.0000	1.0000	1.0000	1.0000	1.0000	1.0000	1.0000	1.0000
798	1.0000	1.0000	1.0000	1.0000	1.0000	1.0000	1.0000	1.0000	1.0000	1.0000	1.0000
799	1.0000	1.0000	1.0000	1.0000	1.0000	1.0000	1.0000	1.0000	1.0000	1.0000	1.0000
800	1.0000	1.0000	1.0000	1.0000	1.0000	1.0000	1.0000	1.0000	1.0000	1.0000	1.0000
801	1.0000	1.0000	1.0000	1.0000	1.0000	1.0000	1.0000	1.0000	1.0000	1.0000	1.0000
802	LAYER 29										
803	1.0000	1.0000	1.0000	1.0000	1.0000	1.0000	1.0000	1.0000	1.0000	1.0000	1.0000
804	1.0000	1.0000	1.0000	1.0000	1.0000	1.0000	1.0000	1.0000	1.0000	1.0000	1.0000
805	1.0000	1.0000	1.0000	1.0000	1.0000	1.0000	1.0000	1.0000	1.0000	1.0000	1.0000
806	1.0000	1.0000	1.0000	1.0000	1.0000	1.0000	1.0000	1.0000	1.0000	1.0000	1.0000
807	1.0000	1.0000	1.0000	1.0000	1.0000	1.0000	1.0000	1.0000	1.0000	1.0000	1.0000
808	1.0000	1.0000	1.0000	1.0000	1.0000	1.0000	1.0000	1.0000	1.0000	1.0000	1.0000
809	LAYER 30										
810	1.0000	1.0000	1.0000	1.0000	1.0000	1.0000	1.0000	1.0000	1.0000	1.0000	1.0000
811	1.0000	1.0000	1.0000	1.0000	1.0000	1.0000	1.0000	1.0000	1.0000	1.0000	1.0000
812	1.0000	1.0000	1.0000	1.0000	1.0000	1.0000	1.0000	1.0000	1.0000	1.0000	1.0000
813	1.0000	1.0000	1.0000	1.0000	1.0000	1.0000	1.0000	1.0000	1.0000	1.0000	1.0000
814	1.0000	1.0000	1.0000	1.0000	1.0000	1.0000	1.0000	1.0000	1.0000	1.0000	1.0000
815	1.0000	1.0000	1.0000	1.0000	1.0000	1.0000	1.0000	1.0000	1.0000	1.0000	1.0000

RECURRENT DATA SET

INITIAL TIME STEP SIZE = 0.00000E+05
 MINIMUM TIME STEP SIZE = 3000.0
 MAXIMUM WATER SATURATION CHANGE = 0.10000
 TIME STEP MULTIPLIER = 1.2500
 TIME TO READ NEW RECURRENT DATA = 0.10000E+17
 NUMBER OF SOURCE/SINK BLOCKS = 0
 CODE FOR CHANGING FLUX RATES = 0

TIME STEP NUMBER = 1 TIME VALUE = 0.00000E+06

CONSTANT PRES	WATER BALANCE	NAPL BALANCE
SOURCE/SINKS	0.00000E+00	0.00000E+00
STORAGE	-2.7884	0.00000E+00
PER CENT ERROR	0.34231E-06	0.00000E+00

STEP NUMBER 1 COMPLETED SIMULATION TIME IN SECONDS 0.0000E+06
 IN MINUTES 0.166E+06
 IN HOURS 240.
 IN DAYS 10.00
 IN YEARS 0.274E-01

TIME STEP NUMBER = 2 TIME VALUE = 0.16660E+07

CONSTANT PRES	WATER BALANCE	NAPL BALANCE
SOURCE/SINKS	0.00000E+00	0.00000E+00
STORAGE	-2.7872	0.00000E+00
PER CENT ERROR	-0.77121E-07	0.00000E+00

STEP NUMBER 2 COMPLETED SIMULATION TIME IN SECONDS 0.166E+07
 IN MINUTES 0.274E+06
 IN HOURS 840.
 IN DAYS 35.0
 IN YEARS 0.81E-01

TIME STEP NUMBER = 3 TIME VALUE = 0.33320E+07

CONSTANT PRES	WATER BALANCE	NAPL BALANCE
SOURCE/SINKS	0.00000E+00	0.00000E+00

Listing of STROUT at 02:22:38 on FEB 5, 1988 for CcId=BEHR on UALTAMS

2481	LAYER 12	734.17	734.96	735.29	737.82	738.98	740.25	741.62	742.97	744.34
2482	733.97	744.11	744.82	746.88	747.31	747.03	747.75	748.62	748.27	748.43
2483	743.42	748.58	748.81	748.82	748.98	748.88	748.55	748.68	748.87	748.87
2484	748.51	748.58	748.58	748.58	748.58	748.58	748.72	748.72	748.71	748.62
2485	748.58	748.88	748.88	748.88	748.88	750.04	750.35	750.72	751.23	751.82
2486	748.61	748.07	748.31	748.57	748.81	750.04	750.35	750.72	751.23	751.82
2487	748.61	748.35	748.72	748.08	748.38	748.72	748.08	748.38	748.72	748.38
2488	LAYER 13	734.41	735.40	735.74	738.07	738.40	740.73	742.07	743.41	744.75
2489	734.41	744.55	747.07	747.45	747.77	748.00	748.28	748.55	748.84	748.00
2490	748.48	748.88	748.08	748.08	748.08	748.10	748.10	748.10	748.11	748.11
2491	748.05	748.08	748.12	748.12	748.12	748.12	748.12	748.12	748.12	748.12
2492	748.12	748.12	748.12	748.12	748.12	748.12	748.12	748.12	748.12	748.12
2493	748.22	748.38	748.87	748.88	748.88	748.88	748.88	748.88	748.88	748.88
2494	748.22	748.82	748.18	748.18	748.22	748.22	748.18	748.18	748.22	748.22
2495	LAYER 14	735.05	735.88	737.18	738.51	738.84	741.17	742.51	743.85	745.22
2496	734.88	747.00	747.82	747.48	748.22	748.48	748.74	748.98	749.22	749.48
2497	748.05	748.08	748.12	748.12	748.12	748.12	748.12	748.12	748.12	748.12
2498	748.58	748.88	748.88	748.88	748.88	748.88	748.88	748.88	748.88	748.88
2499	748.58	748.88	748.88	748.88	748.88	748.88	748.88	748.88	748.88	748.88
2500	748.58	748.88	748.88	748.88	748.88	748.88	748.88	748.88	748.88	748.88
2501	748.58	748.88	748.88	748.88	748.88	748.88	748.88	748.88	748.88	748.88
2502	LAYER 15	735.25	735.49	735.28	737.82	738.98	740.25	741.61	742.96	744.28
2503	735.25	747.44	747.98	748.24	748.52	748.82	749.21	749.50	749.87	749.87
2504	748.74	748.74	748.74	748.74	748.74	748.74	748.74	748.74	748.74	748.74
2505	748.87	748.87	748.87	748.87	748.87	748.87	748.87	748.87	748.87	748.87
2506	748.05	748.05	748.05	748.05	748.05	748.05	748.05	748.05	748.05	748.05
2507	748.12	748.12	748.12	748.12	748.12	748.12	748.12	748.12	748.12	748.12
2508	748.22	748.70	748.70	748.70	748.70	748.70	748.70	748.70	748.70	748.70
2509	LAYER 16	735.73	735.92	735.72	738.08	738.38	740.72	742.05	743.38	744.73
2510	735.73	747.16	748.40	748.78	749.11	749.38	749.65	749.92	750.19	750.46
2511	747.16	747.41	747.41	747.42	747.42	747.42	747.42	747.42	747.42	747.42
2512	747.41	747.45	747.45	747.45	747.45	747.45	747.45	747.45	747.45	747.45
2513	747.45	747.45	747.45	747.45	747.45	747.45	747.45	747.45	747.45	747.45
2514	747.45	747.47	747.47	747.47	747.47	747.47	747.47	747.47	747.47	747.47
2515	747.47	747.47	747.47	747.47	747.47	747.47	747.47	747.47	747.47	747.47
2516	LAYER 17	736.17	736.37	737.17	738.50	738.82	741.15	742.48	743.81	745.14
2517	736.17	748.32	748.84	749.22	749.54	749.82	749.82	749.82	749.82	749.82
2518	747.82	748.32	748.84	749.22	749.54	749.82	749.82	749.82	749.82	749.82
2519	747.82	748.32	748.84	749.22	749.54	749.82	749.82	749.82	749.82	749.82
2520	747.82	748.32	748.84	749.22	749.54	749.82	749.82	749.82	749.82	749.82
2521	747.82	748.32	748.84	749.22	749.54	749.82	749.82	749.82	749.82	749.82
2522	747.82	748.32	748.84	749.22	749.54	749.82	749.82	749.82	749.82	749.82
2523	LAYER 18	736.81	737.61	738.94	740.27	741.60	742.94	744.27	745.60	746.94
2524	736.81	748.78	749.28	749.58	749.87	750.16	750.45	750.74	751.03	751.32
2525	748.08	748.30	748.30	748.30	748.30	748.30	748.30	748.30	748.30	748.30
2526	748.30	748.30	748.30	748.30	748.30	748.30	748.30	748.30	748.30	748.30
2527	748.32	748.32	748.32	748.32	748.32	748.32	748.32	748.32	748.32	748.32
2528	748.32	748.32	748.32	748.32	748.32	748.32	748.32	748.32	748.32	748.32
2529	748.32	748.32	748.32	748.32	748.32	748.32	748.32	748.32	748.32	748.32
2530	LAYER 19	737.25	738.05	739.38	740.71	742.04	743.38	744.71	746.04	747.37
2531	737.25	748.20	748.71	749.04	749.34	749.64	749.94	750.24	750.54	750.84
2532	748.80	748.80	748.80	748.80	748.80	748.80	748.80	748.80	748.80	748.80
2533	748.80	748.80	748.80	748.80	748.80	748.80	748.80	748.80	748.80	748.80
2534	748.80	748.80	748.80	748.80	748.80	748.80	748.80	748.80	748.80	748.80
2535	748.80	748.80	748.80	748.80	748.80	748.80	748.80	748.80	748.80	748.80
2536	748.80	748.80	748.80	748.80	748.80	748.80	748.80	748.80	748.80	748.80
2537	LAYER 20	737.49	737.69	738.92	740.25	741.58	742.91	744.24	745.57	746.90
2538	737.49	748.84	749.34	749.64	749.94	750.24	750.54	750.84	751.14	751.44
2539	748.84	748.84	748.84	748.84	748.84	748.84	748.84	748.84	748.84	748.84
2540	748.84	748.84	748.84	748.84	748.84	748.84	748.84	748.84	748.84	748.84
2541	748.84	748.84	748.84	748.84	748.84	748.84	748.84	748.84	748.84	748.84
2542	748.84	748.84	748.84	748.84	748.84	748.84	748.84	748.84	748.84	748.84
2543	748.84	748.84	748.84	748.84	748.84	748.84	748.84	748.84	748.84	748.84
2544	LAYER 21	738.25	738.15	740.48	741.82	743.15	744.48	745.81	747.14	748.47
2545	738.25	748.28	748.78	749.11	749.44	749.77	750.10	750.43	750.76	751.09
2546	748.28	748.28	748.28	748.28	748.28	748.28	748.28	748.28	748.28	748.28
2547	748.28	748.28	748.28	748.28	748.28	748.28	748.28	748.28	748.28	748.28
2548	748.28	748.28	748.28	748.28	748.28	748.28	748.28	748.28	748.28	748.28
2549	748.28	748.28	748.28	748.28	748.28	748.28	748.28	748.28	748.28	748.28
2550	748.28	748.28	748.28	748.28	748.28	748.28	748.28	748.28	748.28	748.28
2551	LAYER 22	738.24	740.04	741.37	742.70	744.03	745.36	746.69	748.02	749.35
2552	738.24	748.04	748.37	748.70	749.03	749.36	749.69	750.02	750.35	750.68
2553	748.04	748.04	748.04	748.04	748.04	748.04	748.04	748.04	748.04	748.04
2554	748.04	748.04	748.04	748.04	748.04	748.04	748.04	748.04	748.04	748.04
2555	748.04	748.04	748.04	748.04	748.04	748.04	748.04	748.04	748.04	748.04
2556	748.04	748.04	748.04	748.04	748.04	748.04	748.04	748.04	748.04	748.04
2557	748.04	748.04	748.04	748.04	748.04	748.04	748.04	748.04	748.04	748.04
2558	LAYER 23	740.12	740.92	742.25	743.58	744.91	746.24	747.57	748.90	750.23
2559	740.12	748.02	748.32	748.62	748.92	749.22	749.52	749.82	750.12	750.42
2560	748.02	748.02	748.02	748.02	748.02	748.02	748.02	748.02	748.02	748.02
2561	748.02	748.02	748.02	748.02	748.02	748.02	748.02	748.02	748.02	748.02
2562	748.02	748.02	748.02	748.02	748.02	748.02	748.02	748.02	748.02	748.02
2563	748.02	748.02	748.02	748.02	748.02	748.02	748.02	748.02	748.02	748.02
2564	748.02	748.02	748.02	748.02	748.02	748.02	748.02	748.02	748.02	748.02
2565	LAYER 24	741.00	741.80	743.13	744.46	745.79	747.12	748.45	749.78	751.11
2566	741.00	748.89	749.39	749.69	749.99	750.29	750.59	750.89	751.19	751.49
2567	748.89	748.89	748.89	748.89	748.89	748.89	748.89	748.89	748.89	748.89
2568	748.89	748.89	748.89	748.89	748.89	748.89	748.89	748.89	748.89	748.89
2569	748.89	748.89	748.89	748.89	748.89	748.89	748.89	748.89	748.89	748.89
2570	748.89	748.89	748.89	748.89	748.89	748.89	748.89	748.89	748.89	748.89
2571	LAYER 25	742.35	742.55	743.88	745.21	746.54	747.87	749.20	750.53	751.86
2572	742.35	748.39	748.89	749.19	749.49	749.79	750.09	750.39	750.69	750.99
2573	748.39	748.39	748.39	748.39	748.39	748.39	748.39	748.39	748.39	748.39
2574	748.39	748.39	748.39	748.39	748.39	748.39	748.39	748.39	748.39	748.39
2575	748.39	748.39	748.39	748.39	748.39	748.39	748.39	748.39	748.39	748.39
2576	748.39	748.39	748.39	748.39	748.39	748.39	748.39	748.39	748.39	748.39
2577	748.39	748.39	748.39	748.39	748.39	748.39	748.39	748.39	748.39	748.39
2578	LAYER 26	745.88	746.88	747.95	749.32	750.65	751.98	753.31	754.64	755.97
2579	745.88	748.01	748.31	748.61	748.91	749.21				

Appendix 4

Sample calculation - fluid pressure to hydraulic head.

Consider 2 points at the upstream boundary of the flow domain. Both points have water hydraulic heads equal to 625 metres. The upper point (at zero elevation), has a water pressure of 6 125 kPa and the lower point, (295 metres below) has a water pressure of 9 016 kPa. Neglecting capillary forces, (for now) each of these water pressures are converted to hydraulic heads (equation 2.3) by dividing by the specific weight of the oil ($8330 \text{ kg/m}^2/\text{s}^2$). This yields 735.29 and 787.35 metres of oil hydraulic head for the upper and lower points, respectively. Then, a capillary pressure equivalent of 3.6 metres is added, to yield hydraulic heads of 738.89 and 790.95 metres, for the upper and lower points. These are the values observed in Figure 6.4 and in Appendix 3, column 60, layers 1 and 30.